future pharmacology

MDPI

Article

Protective Molecular Mechanisms of Olive Oil Phenolic Compounds: Bioactivity and Pathway Profiling of Isolated Compounds Versus Their Mixture

Sofia I. Prodromou [1,2], Fani Chatzopoulou [3,4], Loukas Kakalis [5], Eleni Kallidou [6], Prokopios Magiatis [7], Vasilis Vasiliou [2] and Ioannis S. Vizirianakis [1,8,*]

[1] Department of Pharmacy, School of Health Sciences, Aristotle University of Thessaloniki, 54124 Thessaloniki, Greece; sofia.prodromou@yale.edu
[2] Department of Environmental Health Sciences, School of Public Health, Yale University, New Haven, CT 06510, USA; vasilis.vasiliou@yale.edu
[3] Department of Biomedical Sciences, School of Health Sciences, International Hellenic University, 57400 Thessaloniki, Greece; fchatzop@auth.gr
[4] Labnet Laboratories, Department of Molecular Biology and Genetics, 54638 Thessaloniki, Greece
[5] Department of Telecommunications, School of Electrical and Computer Engineering, Aristotle University of Thessaloniki, 54124 Thessaloniki, Greece; loukaskakales@gmail.com
[6] Cyprus International Institute for Environmental and Public Health, Cyprus University of Technology, Limassol CY-3036, Cyprus; elenikallidou97@gmail.com
[7] Laboratory of Pharmacognosy and Natural Products Chemistry, School of Pharmacy, National and Kapodistrian University, 15772 Athens, Greece; prokopios.magiatis@gmail.com
[8] Department of Health Sciences, School of Health and Life Sciences, University of Nicosia, Nicosia CY-1700, Cyprus
* Correspondence: ivizir@pharm.auth.gr

Abstract

Introduction: The Mediterranean diet is consistently associated with a reduced risk of chronic diseases, including cancer, cardiovascular disorders, and neurodegenerative conditions. These protective effects are largely attributed to its high intake of plant-derived bioactive compounds, with extra virgin olive oil serving as the principal source of dietary fat. Olive oil phenolic compounds are recognized as key mediators of the Mediterranean diet's antioxidant, anti-inflammatory, and cytoprotective properties. Since oxidative stress and immune dysregulation are central mechanisms in the development and progression of chronic diseases, understanding the cellular and molecular actions of Mediterranean diet-derived bioactives is of significant relevance. This study aimed to assess the bioactivity and molecular effects of selected olive oil phenolic compounds in comparison to a Custom Mixture formulation in order to correlate the modulation of specific pathways with crucial cellular decisions of pharmacological relevance. **Methods:** The effects of olive oil phenolic compounds were evaluated in HepG2 hepatocellular carcinoma cells and peripheral blood mononuclear cells (PBMCs). Cell viability and proliferation assays were performed, along with targeted molecular profile analysis related to cellular pathways involved in DNA repair, lipid metabolism, oxidative stress, inflammation, and neurotrophic signaling. **Results:** Overall, distinct molecular and bioactivity profiles were observed in HepG2 cells among individual phenolic compounds as well as in comparison to their mixture, referring mainly to DNA damage gene response activation (API 1), enhanced antioxidant gene expression (API 7), and apoptosis induction (APIs 5 and 6). Interestingly in PBMCs, combined effects on immune-related and neuroprotective signaling pathways were revealed, alongside the modulation of inflammation-associated gene biomarkers. **Discussion:** As a matter of fact, by affecting proliferation-related and immune response-associated molecular pathways in a cell-specific manner, olive oil phenolic data may represent a mechanistic link between olive oil consumption and chronic disease risk prevention and management in populations.

Check for updates

Received: 9 September 2026
Revised: 8 October 2026
Accepted: 20 October 2026
Published: 29 October 2026

Copyright: © 2026 by the authors. Licensee MDPI, Basel, Switzerland. This article is an open access article distributed under the terms and conditions of the Creative Commons Attribution (CC BY) license.

Keywords: olive oil; phenolic compounds; cytoprotection; HepG2; PBMC; oxidative stress; mixture; molecular pathways

1. Introduction

The Mediterranean diet is widely recognized for its protective role against chronic diseases, including cardiovascular disorders, neurodegenerative conditions, and cancer [1]. These health benefits are attributed to its characteristic dietary pattern, which emphasizes plant-based foods, moderate fish intake, and the use of extra virgin olive oil (EVOO) as the principal source of dietary fat. Among the components of the Mediterranean diet, EVOO plays a central role in mediating disease-preventive effects due to its content of bioactive phenolic compounds, which typically range from 50 to 800 mg/kg in commercial EVOO and may exceed 1000 mg/kg in high-phenolic varieties [2–4]. EVOO phenolics such as oleocanthal, tyrosol, hydroxytyrosol, oleuropein aglycon, ligstroside aglycon, and related secoiridoid derivatives including elenolic acid have been extensively studied for their contribution to the biological activity of the Mediterranean diet [5–9]. These compounds exert diverse pharmacological effects through well-characterized molecular mechanisms, supporting the notion that olive oil phenolics represent key functional constituents of the Mediterranean dietary pattern.

Chronic diseases such as cardiovascular conditions, neurodegenerative disorders, and cancer are closely linked to oxidative stress, which results from an imbalance between reactive species (RS) and the body's antioxidant defenses. The Mediterranean diet, through its high phenolic content—especially from EVOO—has been shown to counteract oxidative stress by scavenging RS and enhancing endogenous antioxidant systems [2,10–12]. This contributes to the modulation of oxidative stress biomarkers and a subsequent reduction in chronic disease risk [13–15].

Within this dietary framework, EVOO phenolics significantly benefit cardiovascular health by enhancing endothelial function and mitigating oxidative injury [14,16–18]. Oleocanthal, one of the most extensively studied EVOO phenolics, exhibits potent anti-inflammatory and anti-cancer properties. Its well-known COX-1 and COX-2 inhibitory activity, comparable to ibuprofen, has been demonstrated in vitro at concentrations of 10–25 μM [19,20]. Beyond its anti-inflammatory profile, oleocanthal induces apoptosis and suppresses proliferation in several cancer models, including breast, prostate, and liver cancer cells, typically within the 10–20 μM range [20–25]. In hepatocellular carcinoma specifically, oleocanthal reduces viability in HepG2 and Hep3B cells at 10–50 μM, promoting lysosomal membrane permeabilization and caspase-dependent apoptosis [21,22]. These findings support its relevance as a dietary phenolic with mechanistic implications for cancer prevention.

Hydroxytyrosol, another key phenolic compound, is recognized as one of the most potent natural antioxidants identified in the Mediterranean diet. In hepatic and endothelial cell models, hydroxytyrosol enhances antioxidant enzyme expression, including SOD and CAT, at 10–100 μM, thereby strengthening endogenous defense systems [26–29]. Its neuroprotective effects have been demonstrated in neuronal and neuroblastoma models at 10–50 μM, where it increases BDNF expression and protects against oxidative injury [28,30]. Hydroxytyrosol also exhibits anti-cancer activity, inducing cell cycle arrest and apoptosis in colon, breast, and prostate cancer cells at 25–100 μM [31,32]. These concentration-dependent effects highlight its broad therapeutic potential across oxidative stress- and inflammation-related pathologies. Oleuropein aglycon, another major secoiridoid derivative, contributes to cardiovascular protection by reducing LDL oxidation and improving HDL functionality

at concentrations of 10–50 μM in endothelial and macrophage models [16,33]. Its anti-inflammatory effects, including downregulation of TNF-α and IL-6, have been observed in vitro at 20–50 μM [34,35]. Oleuropein aglycon also demonstrates anti-cancer properties, inducing apoptosis and inhibiting angiogenesis in breast, colon, and prostate cancer cells at 20–100 μM [22,29,36]. These mechanistic actions underscore this compound relevance as a multifunctional phenolic compound within the Mediterranean diet.

Other EVOO phenolics like tyrosol and elenolic acid also play complementary roles. Tyrosol exerts antioxidant and anti-inflammatory effects in endothelial and hepatic models at 10–50 μM while demonstrating pro-apoptotic activity in hepatocellular carcinoma cells at 25–100 μM [26,28,37]. Elenolic acid, though less extensively studied, exhibits antimicrobial and anti-inflammatory properties in vitro, with emerging evidence suggesting potential synergistic interactions with other secoiridoids [38]. Less studied compounds, such as ligstroside aglycon, have shown anti-cancer effects in cervical and colon carcinoma models at 10–50 μM, supporting its inclusion among bioactive EVOO constituents [39,40].

Recent studies underscore the importance of studying the combined effects of the various bioactive compounds in olive oil, as the synergistic actions of these phenolics can strengthen their biological activities. This may result in more effective regulation of oxidative stress and inflammation, which stems from the Mediterranean diet's bioactivity [41,42]. Notably, the combination of oleocanthal and hydroxytyrosol produces superior anti-inflammatory and cytoprotective effects compared to either compound alone, particularly within the 10–25 μM range [19,20]. However, the molecular mechanisms of such interactions remain largely unclear, especially in complex systems like cancer and immune cells. The diverse phenolic profile of high-phenolic EVOO supports the concept that the therapeutic potential of olive oil is not confined to individual compounds but rather reflects the activity of complex mixtures characteristic of Mediterranean dietary intake [43–45]. Advanced analytical approaches, including two-dimensional mass spectrometry (2D MS/MS) and high-performance liquid chromatography (HPLC–MS), are essential for identifying and characterizing these phenolic profiles and for elucidating their collective bioactivity [46–49].

Olive oil represents a complex biological matrix containing numerous minor constituents that may enhance, attenuate, or mask the effects of individual phenolic compounds. Although several major EVOO phenolics have previously been investigated individually, considerably less is known about how their activities are modified when these compounds are present together in a defined mixture. Therefore, evaluation of the isolated compounds provides an important experimental reference for understanding the biological effects of their combination.

In the present study, we first characterized the cytotoxic and molecular responses induced by selected isolated EVOO phenolic compounds and subsequently compared these responses with those produced by a Custom Mixture designed to reflect the relative occurrence of selected minor constituents within olive oil, rather than to reproduce the complete EVOO matrix. This approach allowed us to examine whether the mixture reproduces, enhances, attenuates, or otherwise modifies the effects observed for its individual constituents. The analysis focused on cellular responses and molecular pathways associated with oxidative stress, DNA repair, neurotrophic signaling, lipid metabolism, and inflammation in HepG2 liver cancer cells and peripheral blood mononuclear cells (PBMCs). Through this comparative approach, we aimed to obtain a more integrated understanding of the biological effects of olive oil phenolics when acting individually and in combination.

2. Materials and Methods

2.1. Cell Cultures

In this investigation, the well-characterized HepG2 human liver cancer cell line (Cellosaurus CVCL_0027; was previously obtained, stored and used in a routine manner in the Laboratory of Pharmacology, School of Pharmacy, Aristotle University of Thessaloniki, Greece, <25 passages were applied), as well as dendritic peripheral blood mononuclear cells (PBMCs) (Human Peripheral Blood-Derived Mature Dendritic Cells, ACF-Cultured, Frozen; STEMCELL Technologies, Thessaloniki, Greece) were used to measure cytotoxicity and molecular profiling. HepG2 cells and PBMCs were frozen at −80 °C until use and were subcultured under controlled conditions (37 °C; humidified atmosphere supplemented with 5% v/v CO_2) in RPMI-1640 medium (Gibco™ RPMI 1640 Medium, Thermo Fisher Scientific, Thessaloniki, Greece). The medium was supplemented with 10%(v/v) fetal bovine serum (FBS) (Gibco™ Fetal Bovine Serum, Thermo Fisher Scientific), penicillin and streptomycin at 100 μg/mL (Gibco™ Pen-Strep, Thermo Fisher Scientific). To maintain logarithmic growth, both cell lines were detached from the culture substrate at approximately 80% confluence, usually every 2–3 days, using trypsin–EDTA (0.25% w/v). The individual olive oil components used in this study were previously prepared, solubilized in DMSO, and stored at 4 °C, and applied identically across experimental treatments for each cell culture as described below. The HepG2 cells were cultured according to previous experimental work [45] and the PBMC line according to manufacturer's guidelines.

2.2. Active Olive Oil Constituents Under Investigation

Eight isolated constituents of olive oil were evaluated in this study (Table 1). The compounds were selected according to their established or putative molecular activities reported in the literature. Five compounds were selected based on well-established bioactive properties, whereas the remaining compounds were included based on molecular effects proposed from their chemical structures. The compounds were isolated at the Laboratory of Pharmacognosy and Natural Products Chemistry, Department of Pharmacy, National and Kapodistrian University of Athens, Greece, using liquid chromatography [50], and subsequently provided to our laboratory for pharmacological evaluation. All isolated constituents used in the present study were of high purity, as established during their isolation and characterization according to the methodology described in Ref. [50].

Table 1. Specifications of the isolated olive oil constituents used in this study.

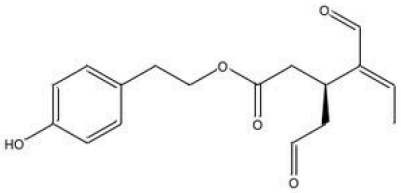
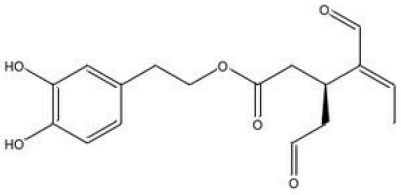
Compound	API Number Used in Testing	Structure	Molecular Weight (g/mol)
Oleocanthal	API 1		304.34
Oleacein	API 2		320.30

Table 1. *Cont.*

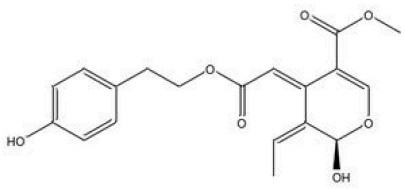
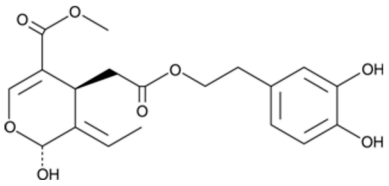
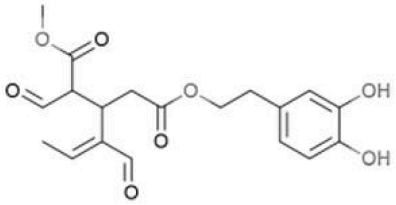
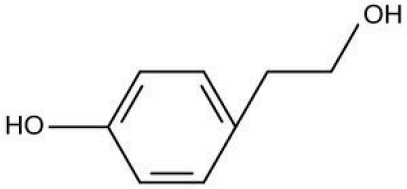
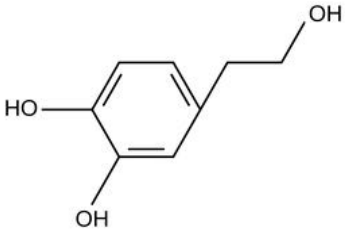
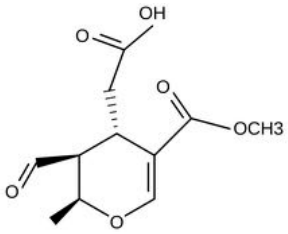
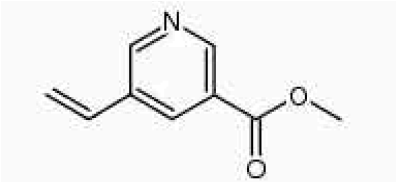
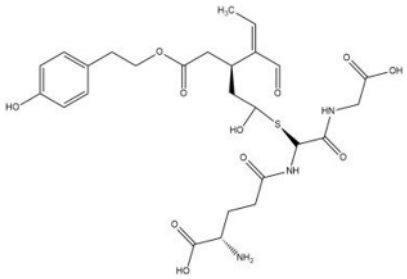
Compound	API Number Used in Testing	Structure	Molecular Weight (g/mol)
Ligstroside ag.	API 3		362.40
Oleuropein aglycone	API 4		378.38
Oleomissional	API 5		378.38
Tyrosol	API 6		138.17
Hydroxytyrosol	API 7		154.17
Elenolic acid	API 8		242.22
5-Vinyl-3-pyridinecarboxylic acid methyl ester	API 9		163.17

Table 1. *Cont.*

Compound	API Number Used in Testing	Structure	Molecular Weight (g/mol)
Oleoglutathione	API 10		597.20

For consistency with the experimental coding system used throughout the study, the investigated olive oil constituents were assigned identifiers API 1–11. In the present manuscript, "API" is used solely as an experimental sample code and does not denote an active pharmaceutical ingredient.

In addition to the isolated compounds, a defined formulation of selected olive oil minor constituents, referred to as the Custom Mixture (API 11), was evaluated. The mixture was provided already prepared by the Laboratory of Pharmacognosy and Natural Products Chemistry, Department of Pharmacy, National and Kapodistrian University of Athens, Greece and was formulated according to the previously established isolation and characterization process described in Ref. [50]. The formulation contained APIs 1–8 together with two additional isolated compounds (APIs 9 and 10, which were not individually evaluated in the present study). Importantly, the constituents were not combined in arbitrary or equimolar proportions. Instead, their relative proportions were selected to reflect the naturally occurring compositional pattern of these phenolic constituents in olive oil. Thus, the Custom Mixture was intended to provide a defined experimental formulation reflecting the relative composition of selected olive oil minor constituents. It was not designed to reproduce the complete olive oil matrix, particularly its predominant lipid fraction, and enables comparison of the biological responses produced by the combined constituents with those observed for the individually evaluated compounds.

2.3. Cell Propagation in Established Cell Lines and Cytotoxicity Assessment

Cytotoxicity was determined using the Dojindo Cell Counting Kit-8 (CCK-8) (Dojindo Molecular Technologies, Munich, Germany), an approved method for cell viability analysis, in HepG2 cell lines. For a standard cytotoxicity assay, HepG2 cells were grown at a density of 8×10^3 cells/mL into 96-well plates (Corning Costar, New York, NY, USA) in a CO_2 incubator for 24 h to allow for cell attachment, before treatment with the test agents (isolated olive oil subfractions). API solutions were diluted to final concentrations of 1, 10 and 50 µM and incubated with cells at 37 °C in a 5% CO_2 incubator for 24 h. At the end of each treatment period, the treatment-containing medium was completely aspirated from the wells. As HepG2 cells remained adherent to the culture surface, the cells were subsequently washed with PBS to remove residual treatment compounds. Fresh treatment-free culture medium containing the CCK-8 reagent was then added, and absorbance was measured according to the assay protocol. Untreated cells cultured in medium and subjected to the same washing and CCK-8 procedure served as the control. This procedure ensured that the CCK-8 reaction and subsequent absorbance measurement were performed after removal of the phenolic-containing treatment medium, thereby minimizing potential direct interference of the investigated compounds with the colorimetric readout.

The levels of cell toxicity were determined and expressed as a percentage of untreated control cells. Absorbance values at 450 nm were taken as indices of formazan product levels (indicating cell viability). Control wells were prepared under the same conditions

but contained only culture media without treatment. For time-dependent toxicity, all APIs were tested at 50 μM for exposure times between 24 and 120 h, and viability was measured at 24 h intervals. Cytotoxicity was reported at the percentage of cell viability, both dose- and time-dependent [45]. The concentration ranges tested did not generate complete dose–response curves suitable for reliable nonlinear regression and IC_{50} calculation.

Cell growth was also evaluated with a Neubauer counting chamber under the microscope for each API as a separate experiment. For adherence, HepG2 cells were plated at 8×10^3 cells/mL in RPMI-1640 media overnight and then cells cultures were exposed for the period of 24–120 h with the maximum concentration of each API (50 μM). Trypan Blue staining (Gibco™ Trypan Blue, Thermo Fisher Scientific) was performed to assess cell death. At the end of the treatment period, cells were detached through trypsinization according to standard protocol and cell counts were compared with controls. Treatments were performed in triplicate for reliability. Control wells were set up using the same experimental conditions.

2.4. Ki-67 Proliferation Marker Detection Using Confocal Microscopy

A specific protocol was followed for detecting Ki-67 to assess cell proliferation in HepG2 cells. Briefly, 1.5×10^4 cells in 1 mL of culture medium were seeded onto Matrigel-coated glass coverslips (12 mm diameter) in a 24-well tissue culture plate. After the cells had adhered for 24 h, the test APIs were added at the highest concentration (50 μM) according to the CCK-8 assay. The cells were incubated for 24 h for proliferation.

After 24 h of incubation, the media was removed, and the cells were fixed in 300 μL of 4% paraformaldehyde (PFA) for 20 min at RT. Fixed cells were washed twice for 5 min with cold 1× PBS to remove excess fixative. Coverslips were then moved to a new 24-well plate, and the cells were permeabilized with 400 μL of 0.1% Triton X-100 lysis buffer for 10 min. For immunostaining 250 μL of primary rabbit anti-Ki-67 antibody D3B5 mAb (Alexa Fluor 647 Conjugated) (Cell Signaling Technology, Athens, Greece) was diluted in 10% normal goat serum (NGS) (v/v) and a ratio of 1:1000 (v/v) was added to each well and kept bronzed 3 h at 37 °C and protected from light with aluminum foil. The wells were washed three times with 300 μL of 1× PBS to remove unbound antibody after staining, and the nuclei were counterstained with 300 μL of DAPI (Invitrogen™ DAPI and Hoechst Nucleic Acid Stains, Fisher Scientific, Athens, Greece) for 10 min at room temperature. Any excess DAPI was removed by three 300 μL washes with 1× PBS.

The stained coverslips were then mounted on glass slides (using miscible immersion oil) and covered with a micro cover glass. Fluorescent signals were observed and analyzed with the Nikon Eclipse E600 confocal microscope (Nikon, Tokyo, Japan), and Ki-67 was captured at 450–520 nm and DAPI at 330–420 nm. At least 1000 cells were counted per sample, and all data shown represent the means from three independent experiments. Cellular structure was assessed through the use of an upright microscope, which would give high-resolution imaging of cell morphology and structural components. This arrangement allowed efficient visualization of cell shape, size, and structural alterations induced by experimental treatments.

2.5. RNA Isolation and Real-Time Quantitative Polymerase Chain Reaction (qPCR)

To analyze gene expression and gain further insight into the potential effects of APIs 1–8, cells were incubated for molecular analysis of gene expression after conducting the aforementioned experiments. The concentration of 50 μM was chosen (the highest concentration tested) and the cells were incubated for 48 h to help amplify the differences in gene expression. Total RNA was extracted, and the expression of 42 genes associated with hepatotoxicity, DNA repair, neurogenesis, drug metabolism, and oxidative stress was assessed.

Gene expression analysis was performed using custom RT^2 Profiler PCR Array plates (Qiagen, Hilden, Germany). The genes of interest were selected by the authors according to the molecular processes investigated in the study, whereas the corresponding gene-specific primer assays were designed and pre-validated by the manufacturer and supplied pre-dispensed in the custom array plates. Therefore, individual primer sequences were not designed by the authors. RNA was isolated using the RNeasy Plus Micro Kit (Qiagen, Hilden, Germany) [45], and 200 ng of total RNA was used for cDNA synthesis using the QuantiTect Reverse Transcription Kit (Qiagen, Hilden, Germany), according to the manufacturer's instructions. After extraction, the purity of the obtained RNA was ascertained via the Thermo Scientific NanoDrop 2000, USA spectrophotometer (Thermo Fisher Scientific, Athens, Greece).

Gene expression was quantified using the ΔΔCt method. In pursuit of optimal amplification plots within the range of 35 to 40 Ct (Cycle threshold) for each gene under scrutiny, a 1:20 dilution was systematically carried out on samples. Five reference genes included within the array configuration (ACTB, B2M, GAPDH, HPRT1, and RPLP0) were used for normalization in accordance with the Qiagen array workflow. Expression and fold change data, including the reference genes, are provided in the Supplementary (Table S4a,b, S5 and S6). Because very low expression in control samples can result in large calculated fold changes, particularly high fold change values were interpreted cautiously and in the context of the overall expression pattern rather than as direct measures of the magnitude of a biological response.

2.6. Bioinformatic Analysis of the Differentially Expressed Genes Data

Differentially expressed gene data were subjected to bioinformatic analysis to clarify their biological activities and the molecular pathways in which they are involved [45]. The GitHub Copilot—Python Scripts (v 3.15.1) package was used to perform the overrepresentation analysis for Gene ontology (GO) including Biological Process (BP), Molecular Function (MF) and Cellular Component (CC). Pathway analysis was constructed using the Reactome pathway database and Disease Ontology Semantic and Enrichment analysis (DOSE), implemented via Gseapy (v 1.3.1) for gene set enrichment analysis. Pandas (v 3.1.0) was used for data cleaning and preprocessing, while Matplotlib (v 3.11.2) and Seaborn (v 0.13.2) were employed for data visualization in Python. The protein–protein interaction (PPI) network was constructed using the STRING-DB tool (v 12.5) in RStudio (v 2026.10.0).

2.7. Statistical Analysis

All experiments were performed in at least three independent biological replicates. Data were analyzed using standard statistical procedures appropriate for each dataset. Normality was assessed prior to analysis, and parametric or non-parametric tests were applied accordingly. Differences between treatment groups and controls were evaluated using one-way or two-way ANOVA followed by suitable post hoc comparisons and Shapiro–Wilk test for normalization, while time course experiments were analyzed using repeated-measures approaches. Results are presented as mean ± standard deviation (SD), and statistical significance was set at $p < 0.05$. All analyses were conducted using validated statistical software GraphPad Prism V11.0.1.

2.8. Graphical Abstract Preparation Using Generative Artificial Intelligence

The graphical abstract was generated and subsequently refined using ChatGPT (OpenAI, GPT-6), incorporating its AI-based image generation capabilities. The tool was used exclusively for the visual representation of the study design, experimental models, molecular pathways, and principal findings presented in the manuscript. The scientific content and terminology were provided and reviewed by the authors to ensure consistency with

the experimental results. Generative AI was not used to generate, modify, or analyze experimental data or to produce the scientific figures derived from the experiments.

3. Results

3.1. Cytotoxicity Assessment of APIs 1–8

Treatment with APIs 1–8 resulted in distinct effects on HepG2 cell viability and proliferation. These effects varied according to both compound concentration and exposure duration. The concentration-dependent analysis (Figure 1, Tables S1 and S2) was first used to characterize the response of HepG2 cells to increasing concentrations of each individual compound. APIs 1 (oleocanthal) and 7 (hydroxytyrosol) generally maintained cell viability above 50%, APIs 3 (ligstroside aglycon) and 8 (elenolic acid) demonstrated moderate increases, peaking at 30%, whereas APIs 5 (oleomissional) and 6 (tyrosol) produced greater reductions in viability at higher concentrations. API 4 (oleuropein aglycone) showed a biphasic response, with increased proliferation at lower concentrations followed by a more cytostatic response at higher concentrations.

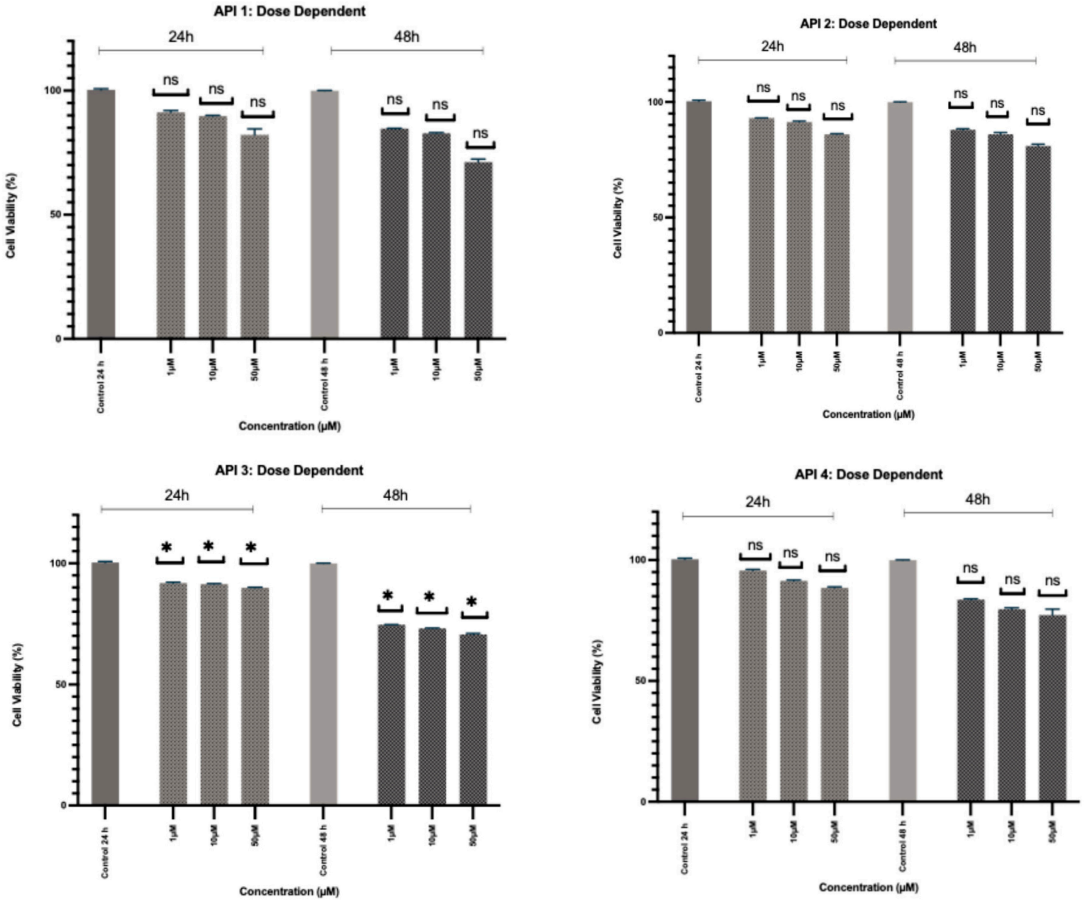


Figure 1. *Cont.*

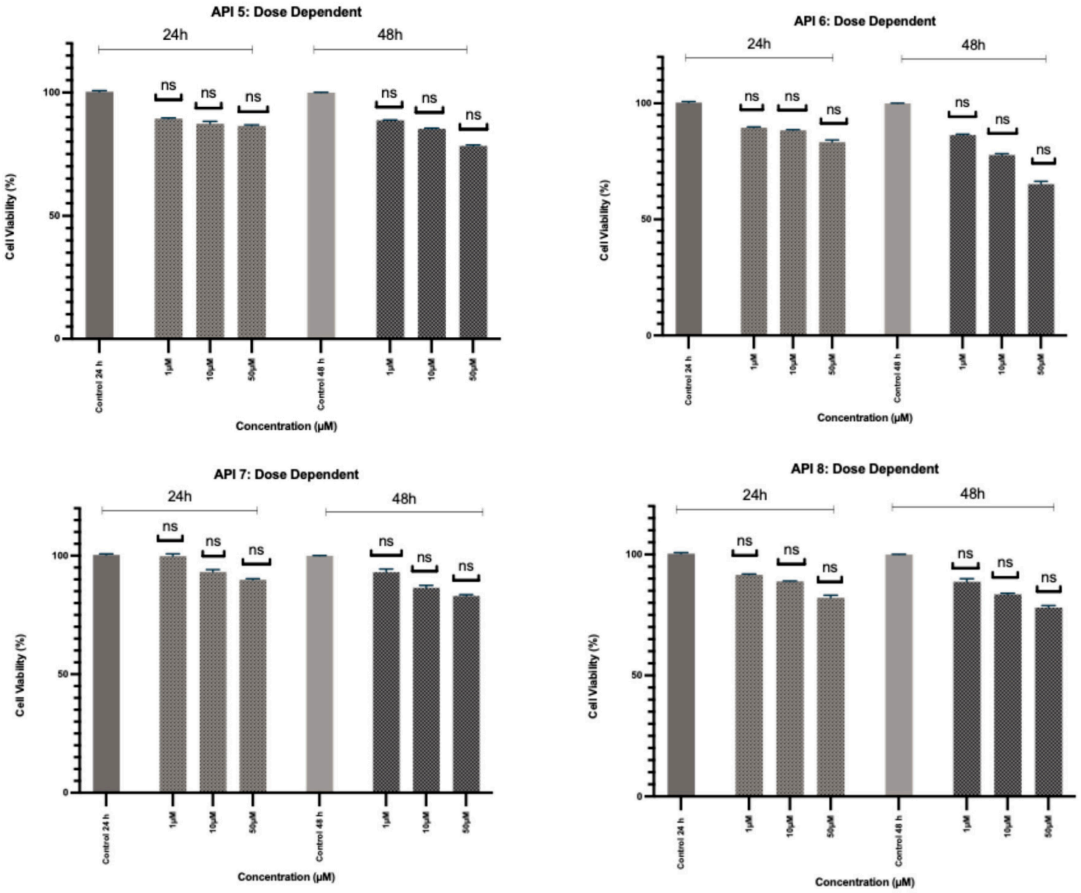


Figure 1. Concentration-dependent assessment of cellular viability of HepG2 cells exposed to APIs 1–8 as measured with the CCK-8 assay (24 and 48 h). The data present statistically significant differences ($p < 0.05$), notably for API 3, compared to different treatments (n = 3). Statistical significance is denoted as follows: * $p < 0.05$ versus [control/specify comparison group]; ns, not significant ($p \geq 0.05$).

The time-dependent analysis (Figure 2) further demonstrated that the cellular responses to the individual phenolics were dynamic. APIs 1 and 7 maintained relatively high cell viability throughout the exposure period, with their greatest effects observed between 72 and 96 h before reaching a plateau at 120 h. APIs 3 and 8 showed their greatest proliferative responses at later time points, approximately 96 h. In contrast, APIs 4, 5, and 6 produced more pronounced decreases in viability, particularly around 72 h, although some recovery was observed at subsequent time points, suggesting cellular adaptations or recovery mechanisms. API 4 eventually broadened to exhibit cytostatic effects by 120 h, and APIs 5 and 6 continue to display decreasing viability, confirming their cytotoxic profiles.

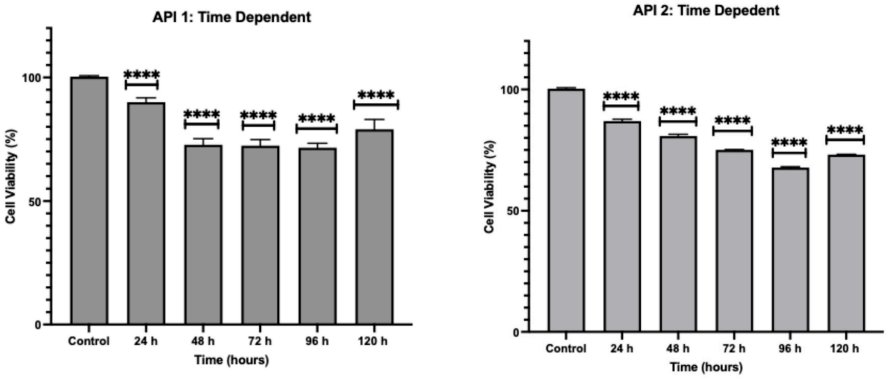


Figure 2. *Cont.*

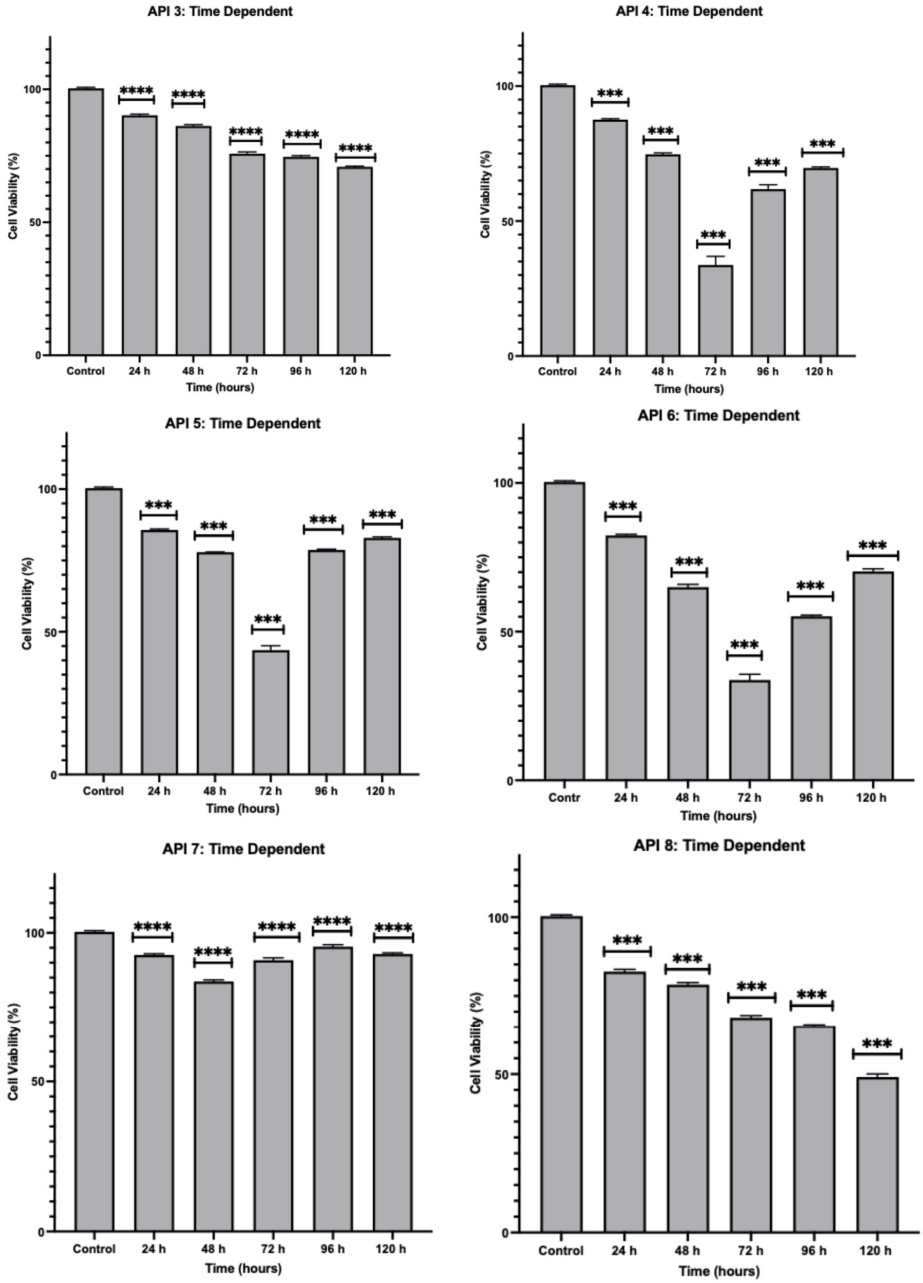


Figure 2. Time-dependent assessment (24–120 h) of cellular viability of HepG2 cells exposed to various treatments of APIs 1–8, as measured with the CCK-8 assay. The data present statistically significant differences ($p < 0.05$) compared to different treatments (n = 3). Statistical significance is denoted as follows: *** $p < 0.001$, **** $p < 0.0001$ versus [control/specify comparison group]; ns, not significant ($p \geq 0.05$).

As for the added cytotoxicity evaluation utilizing the Neubauer counting chamber (Figure 3), the recognized reaction did not exhibit a distinct concentration-dependent pattern. Interestingly, a time-dependent pattern indicated the normal growth cycle of HepG2 cells. Overall, the observations relating to cell growth were consistent with the toxicity data: compounds that drove strong mitogenic effects were associated with substantial cell proliferation and no indications of toxicity, and vice versa for compounds driving weaker mitogenic activity, suggesting a connection between cell proliferation and cytotoxicity.

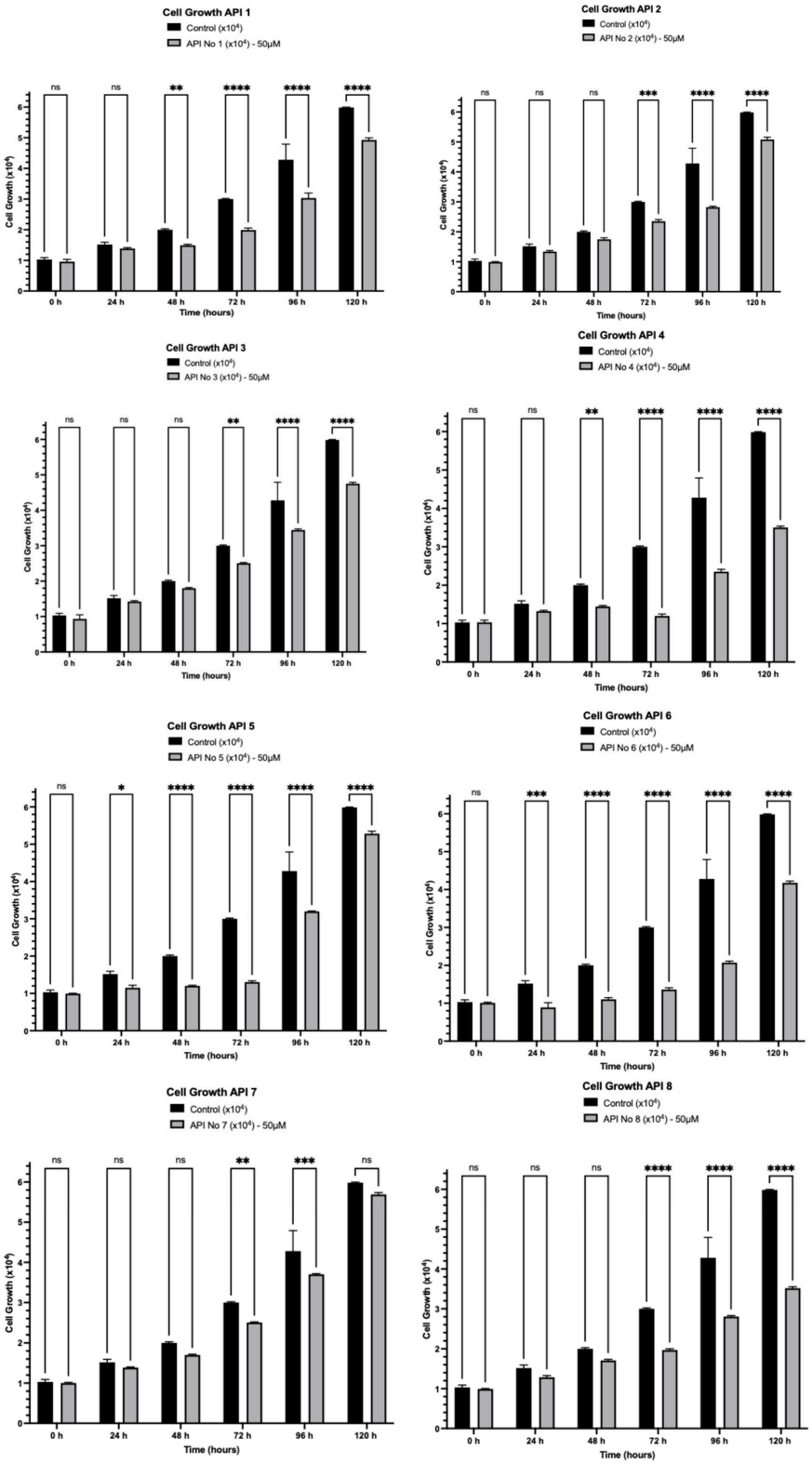
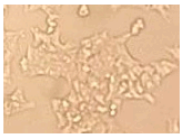
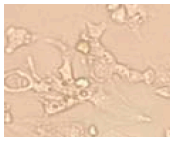
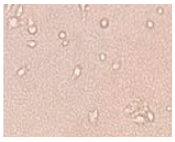
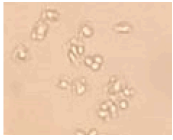
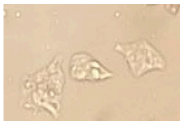


Figure 3. Cell growth and death assessment (24–120 h) of HepG2 cells exposed to various treatments of APIs 1–8, as measured with the Neubauer counting chamber. Data are presented as mean ± SD (n = 3). Statistical comparisons were performed between each API treatment and the corresponding control at each time point. Statistical significance is indicated as follows: ns, not significant; * $p < 0.05$; ** $p < 0.01$; *** $p < 0.001$; **** $p < 0.0001$.

The cellular phenotype (Table 2) was noted and recorded with phase contrast microscopy images of HepG2 cells after treating with APIs 1–8 plus a Custom Mixture,

followed by cell growth and death assessment. Acquired after exposure to the APIs for 120 h, the images provided explicit visual representations of the cellular morphology and evident alterations in size, shape, density, and nuclear character. These images were critical for defining the unique phenotypic response associated with each API treatment, providing insight into the effects of these compounds on cell proliferation, apoptosis, and overall cellular health.

Table 2. Phenotype Images of HepG2 Cells treated with APIs 1–8 and Custom Mixture (120 h exposure). The images present distinct cellular phenotypes of HepG2 cells, captured at a magnification of ×500, and highlight the morphological changes induced by the treatments, including alterations in cell shape, clustering, and nuclear integrity.

	Control	API 1	API 2	API 3	API 4	API 5
Phenotype after 120 h exposure						
	API 6	API 7	API 8	Custom Mixture		
Phenotype after 120 h exposure						

The images shown correspond to small selected areas of the wells and therefore may not fully capture the overall cell phenotype across the entire plate. Variations between the microscopic phenotype and the photometric measurements may arise from this limitation, as the photometric assay integrates signal from the entire well, while the images depict only a localized region.

3.2. Confocal Microscopy Detection of Ki-67 Proliferation Marker of APIs 1–8

Confocal microscopy analysis (Table 3 and Table S3) demonstrated the impact of every active pharmaceutical ingredient on mitosis rate, cellular structure, apoptosis, and cell cycle progression in HepG2 cells. Among the 8 APIs, 1 (oleocanthal) and 7 (hydroxytyrosol) had high mitotic rates, with values close to or over 90%. Confocal images of these treatments showed dense clusters of cells with round, moderate, and healthy cell morphologies, indicative of active cell division. The nuclear structures had no signs of chromatin condensation or fragmentation. Moreover, these APIs showed increased Ki-67 staining, particularly during the S and M phases, indicating their contributions to active cell cycle progression without significantly inducing apoptosis.

In comparison, APIs 5 (oleomissional) and 6 (tyrosol) showed lower mitotic rates (11.1% and 16%, respectively), and thus a practical inhibitory impact on cell proliferation. As seen by confocal microscopy, nuclear condensation and frequent nucleus fragmentation further indicate apoptosis with reduced cell densities. Cells treated with these APIs also exhibited a variety of morphological hallmarks of cytotoxic effects such as irregular shapes, cytoplasmic blebbing and, in some cases, membrane integrity loss. Collectively, these morphological changes indicate that APIs 5 and 6 may cause cell cycle arrest, most likely at the G0/G1 phase, and induce programmed cell death, rather than supporting proliferation, a tendency that seems to be revoked after 96 h of treatment.

API 3 (ligstroside aglycon) also exhibited moderate proliferative action on mitosis, approximately 66.6% and 61.1%, respectively. Confocal imaging showed preserved cell morphologies and moderately increased cell densities; however, some cells exhibited elongated or spindle-shaped forms, suggesting active cell proliferation without excessive mitotic stimulation. Moreover, Ki-67 staining showed increased activity in the G1/S phases, facilitating continuous progression through the cell cycle with minimal signs of apoptosis.

A comparable impact on mitotic activity and cellular structure integrity was found in API 2 (oleacein), API 4 (oleuropein aglycon), and API 8 (elenolic acid); they induced moderate mitotic activity and preserved cellular structure integrity. These APIs resulted in minimal chromatin condensation, intact nuclear membranes, and even distribution through the cell cycle phases.

Table 3. Group of confocal images of HepG2 cells exposed to various treatments of APIs 1–8, as measured with the proliferation marker Ki-67.

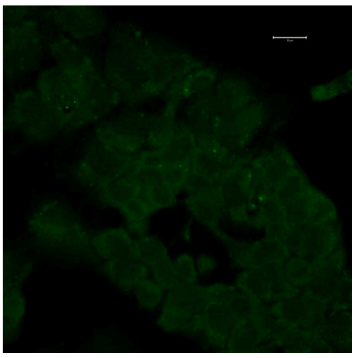
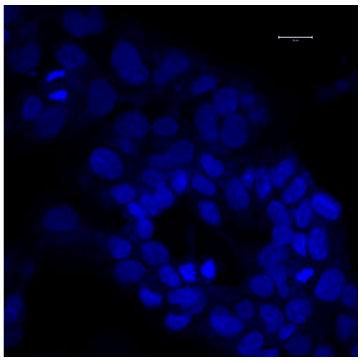
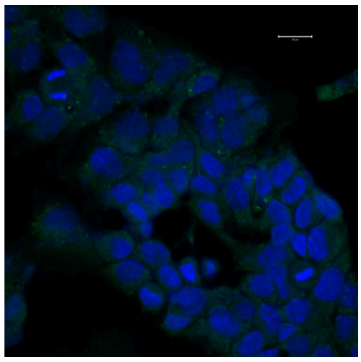
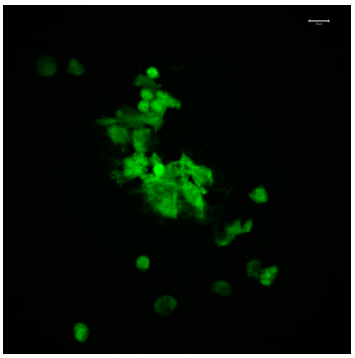
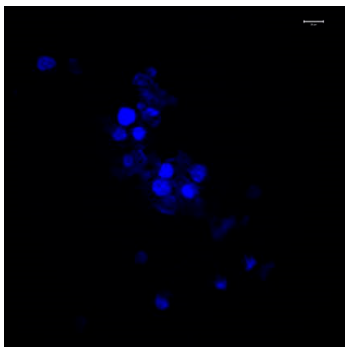
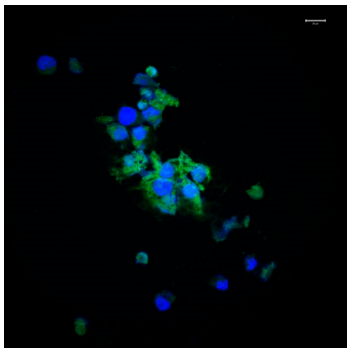
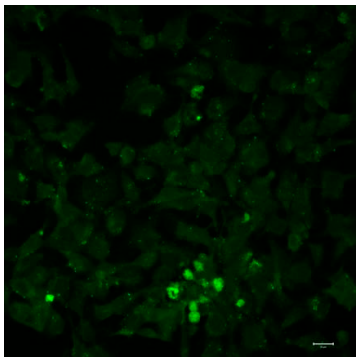
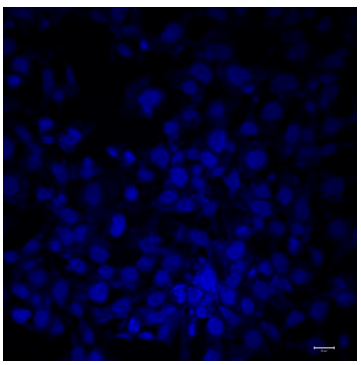
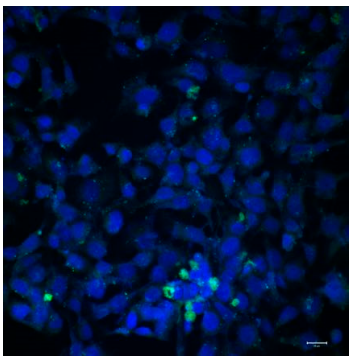
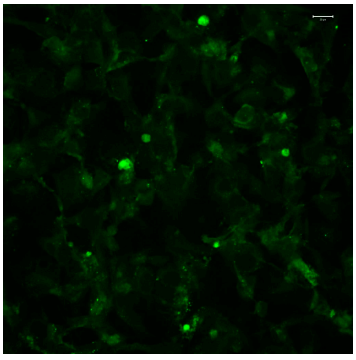
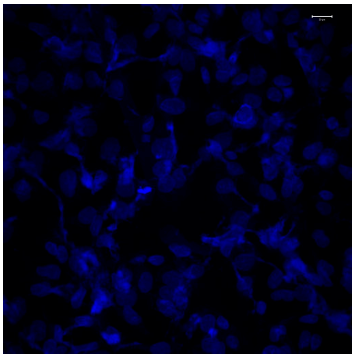
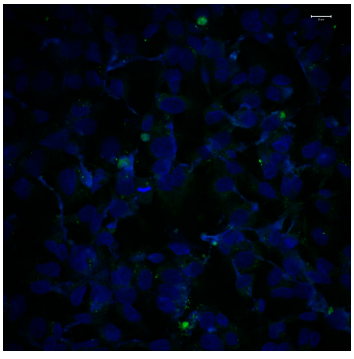
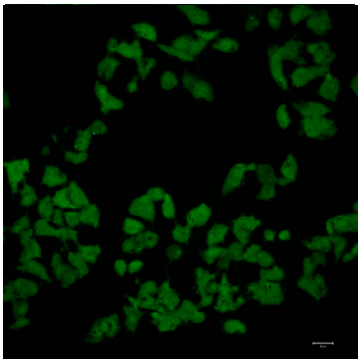
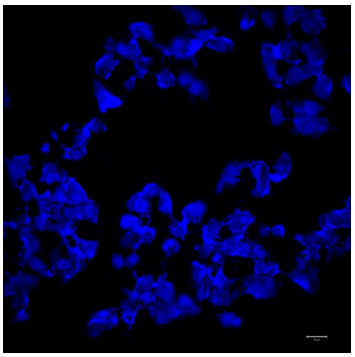
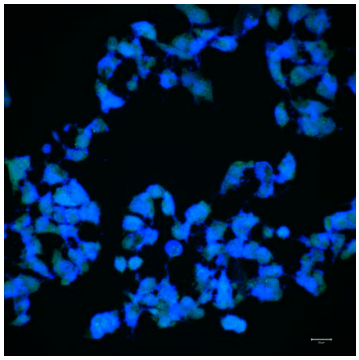
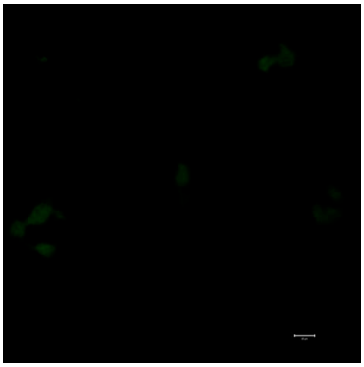
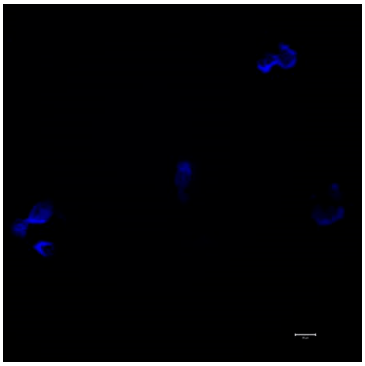
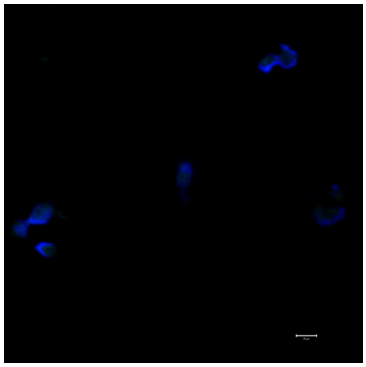
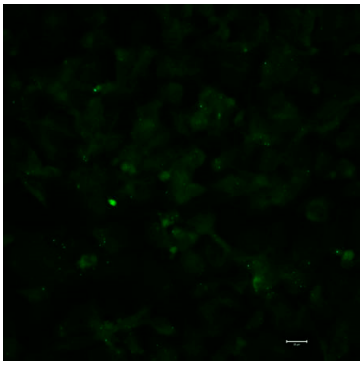
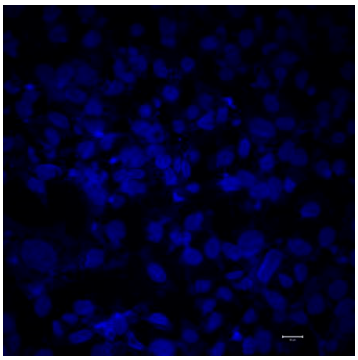
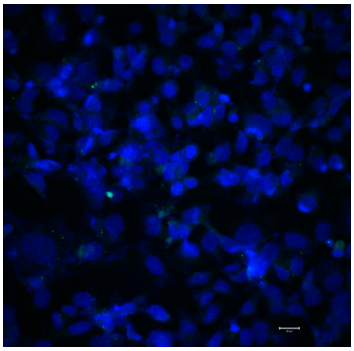
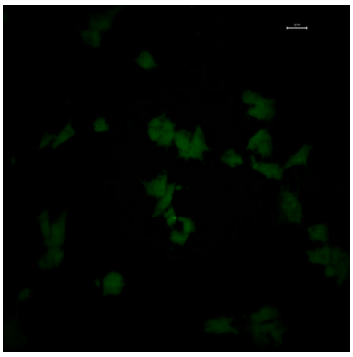
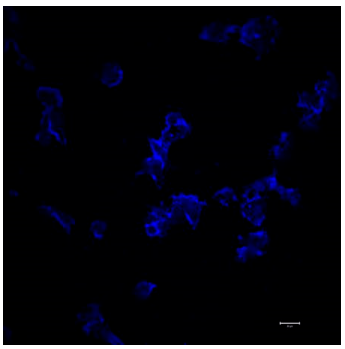
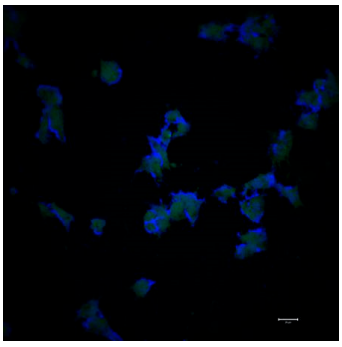
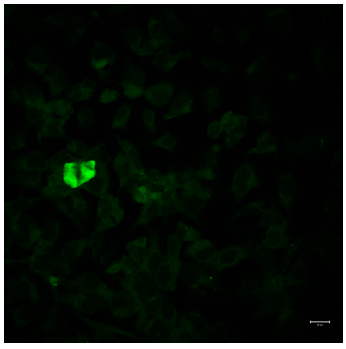
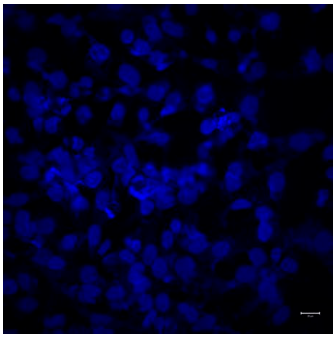
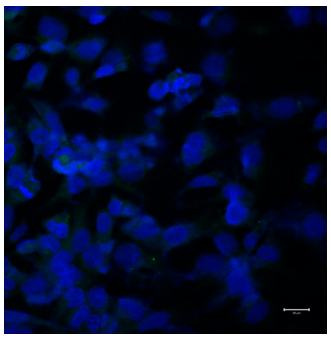
	Ki-67	DAPI	MERGED
Control			
API 1			
API 2			
API 3			

Table 3. *Cont.*

API 4			
API 5			
API 6			
API 7			
API 8			

3.3. Gene Expression Profiling Assessment with the RT2 Profiler PCR Array Using Real-Time Quantitative Polymerase Chain Reaction (RT-PCR) and Bioinformatic Evaluation

To facilitate interpretation of the molecular responses induced by the individual phenolic compounds (Figures 4 and 5), the differentially expressed genes were considered according to their major functional categories: DNA damage and repair, oxidative stress and antioxidant defense, neurotrophic signaling, inflammation and apoptosis, and drug metabolism.

Regarding DNA damage and repair, APIs 1 (oleocanthal) and 7 (hydroxytyrosol) produced pronounced changes in genes involved in genomic maintenance. API 1 markedly increased ATM and APEX1 expression, whereas API 7 also strongly increased APEX1 expression. These findings indicate that the two phenolics influence DNA damage response pathways, although the magnitude and pattern of gene regulation differed between treatments. As shown in Figure 4, APIs 5 (oleomissional) and 6 (tyrosol) showed modest or no upregulation of ATM and XRCC1, consistent with its genomic protective effects, indicating reduced DNA repair activation. Conflicting evidence for genomic stability of cell cycle and DNA repair genes may arise from the pathway enrichment reported for several APIs (1 and 7) related to cell proliferation and genomic stability.

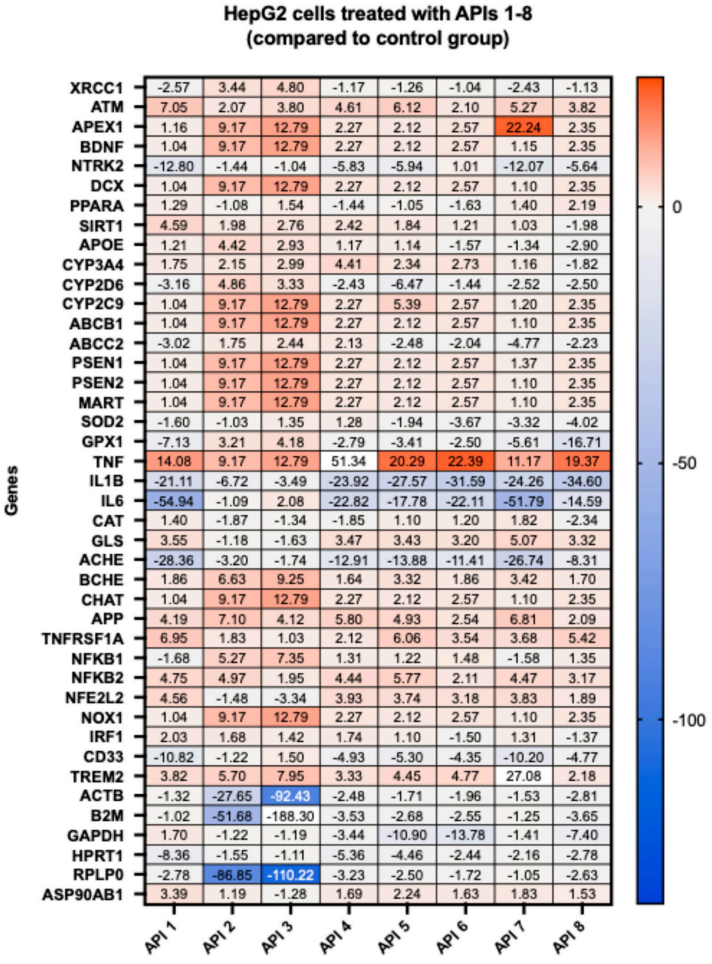


Figure 4. Heatmap representing the differentially expressed genes of HepG2 cells upon treatment with APIs 1-8 compared with untreated control samples. Red indicates the upregulated genes and blue the downregulated genes. The intensity of the color highlights the strength of the regulation.

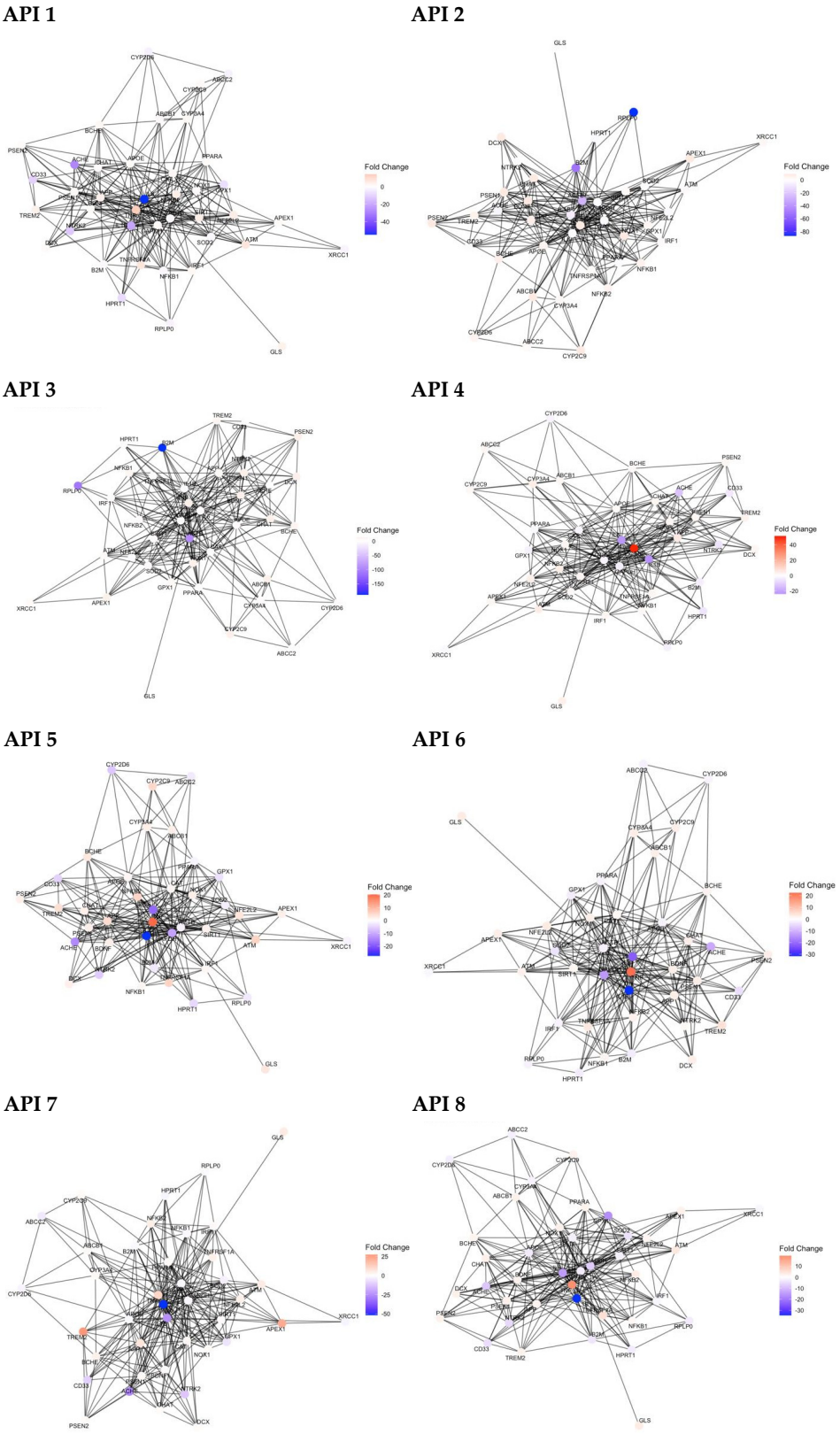


Figure 5. Protein–protein interaction (PPI) network for APIs 1–8. This network visualizes predicted protein–protein interactions among the genes regulated by the specified API. Nodes represent gene-encoded proteins, and edges indicate known or predicted functional associations from the STRING database. Node color reflects the magnitude and direction of fold regulation, with upregulated genes in red, downregulated genes in blue, and white indicating no change.

Regarding oxidative stress and antioxidant defense, APIs 1 and 7 were associated with increased SIRT1 expression, consistent with modulation of cellular stress response pathways. In contrast, APIs 5 and 6 showed reduced expression of antioxidant-associated markers, including CAT and GPX1, which was consistent with their more cytotoxic cellular profiles. The results correlate with pathway enrichment, where APIs 1 and 7 were involved in stress response and metabolic regulation, and APIs 5 and 6 were associated with pro-inflammatory and oxidative damage pathways.

In pathways relating to neurogenesis, API 7 strongly upregulated BDNF and NTRK2, suggesting its neuroprotective potential. In contrast, minor changes were observed for APIs 5 and 6 in markers such as BDNF, highlighting their constrained neurogenic activity. Similarly, API 7 was enriched in pathways related to synovial signaling and neuronal development, while APIs 5 and 6 demonstrated minimal changes in these markers, emphasizing their limited neurogenic activity. Pathway analysis further supported these findings with API 7, which was enriched in synaptic signaling and neuronal development pathways, while APIs 5 and 6 showed weaker associations.

Gene profiles were divergent for inflammation- and apoptosis-related genes. APIs 1 and 7 showed dramatically high TNF expression levels, a marker of inflammatory signaling after cell proliferation. In contrast, downregulated IL6 and IL1B were abundantly expressed in APIs 5 and 6, which underscores their cytotoxic activity and the attenuation of inflammatory pathways. Enrichment analysis revealed that immune response pathways were mainly associated with APIs, especially APIs 5 and 6, suggesting a potential immune modulatory and cytotoxic role.

Regarding metabolic pathways, APIs 3 and 8 had moderate upregulation with increased activity of CYP3A4 and ABCC2. APIs 5 and 6, however, exhibited few changes in drug metabolism-associated genes, commensurate with their decreased cellular viability and cytotoxicity profiles. This was supported by pathway analysis, showing enrichment of APIs 3 and 8 in lipid and metabolic signaling, suggesting functional roles in managing energy and processing nutrients.

In conclusion, these results indicate that APIs 1 and 7 emerged as key players in promoting DNA repair, cell cycle regulation and defense against oxidative stress. The moderate activity of APIs 3 and 8 in metabolic and signaling pathways represented balanced cell growth. In contrast, APIs 5 and 6 exhibited limited protective effects and prominent cytotoxic profiles, highlighting their possible risks. The unique patterns of fold regulation across APIs 1–8 highlight their diverse biological implications, ranging from potent proliferative and protective responses to evident cytotoxic effects.

3.4. Custom Mixture of Olive Oil Results Analysis.

The Custom Mixture exhibited multifaceted effects in HepG2 cells across several disciplines, including cell growth, confocal microscopy, qPCR expression profiles, and cell toxicity. The Custom Mixture has shown moderate effectiveness for cell viability and proliferation compared to individual API treatments.

Regarding cell viability (Figures 6 and 7), the Custom Mixture exhibited a distinct combined effect across the evaluated doses and time points. Cell viability decreased in cells treated with the mixture, especially after 48 h, compared to 24 h, with no significant alterations between the different doses. The mixture preserved viability over time, stabilizing at 120 h without any significant toxicity observed. The findings indicate that the Custom Mixture harnesses complementary mechanisms of its building blocks to promote an advantageous cellular-mediated defense and respond appropriately.

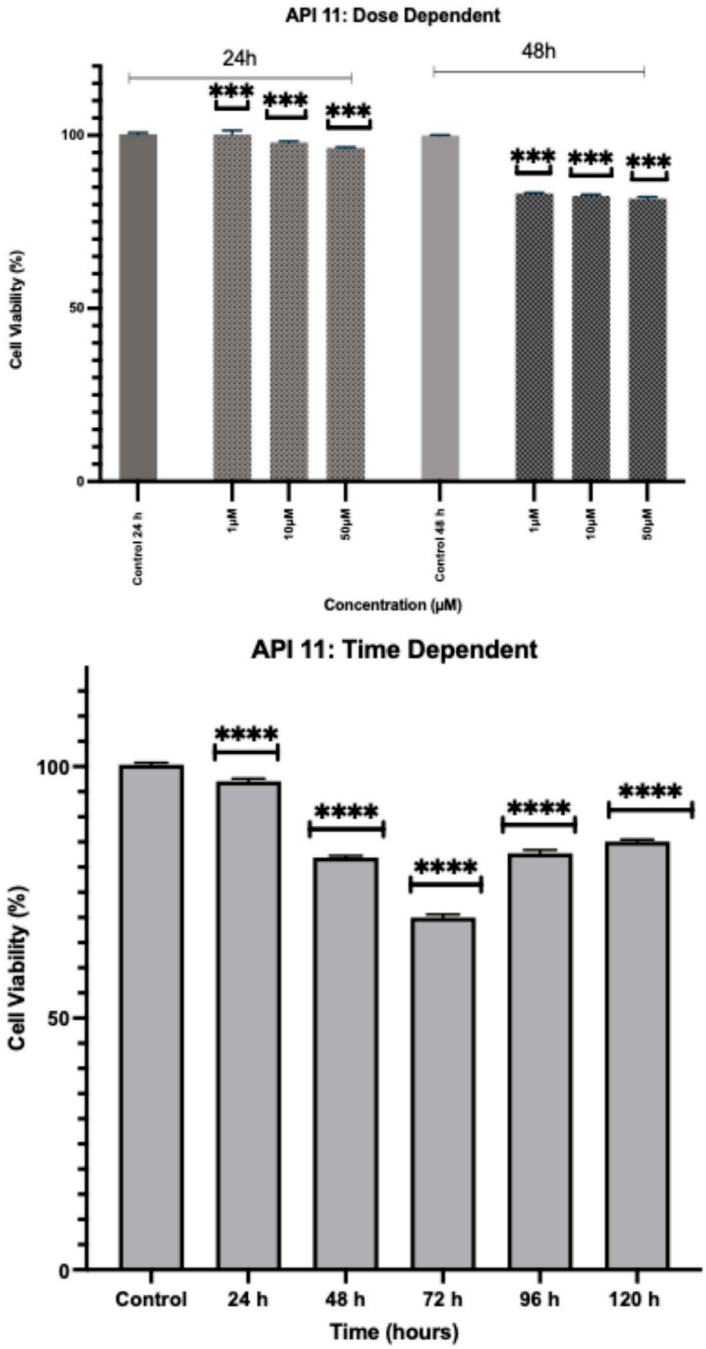


Figure 6. Concentration- and time-dependent assessment of cellular viability of HepG2 cells exposed to Custom Mixture as measured with the CCK-8 assay (24–120 h). The data present statistically significant differences ($p < 0.05$) compared to different treatments (n = 3). Statistical significance is indicated as follows: ns, not significant; *** $p < 0.001$; **** $p < 0.0001$.

Unlike high-mitotic APIs, this combination did not promote cell division. Confocal microscopy (Table 4) confirmed fewer mitotic figures and lower densities of actively dividing cells compared to API 7. Fascinatingly, Custom Mixture treatment was associated with structural preservation together with morphological features suggestive of apoptotic processes, including chromatin condensation and nuclear fragmentation. As apoptosis-specific assays were not performed, these observations were interpreted as morphological evidence of potential apoptotic changes rather than direct confirmation of apoptosis.

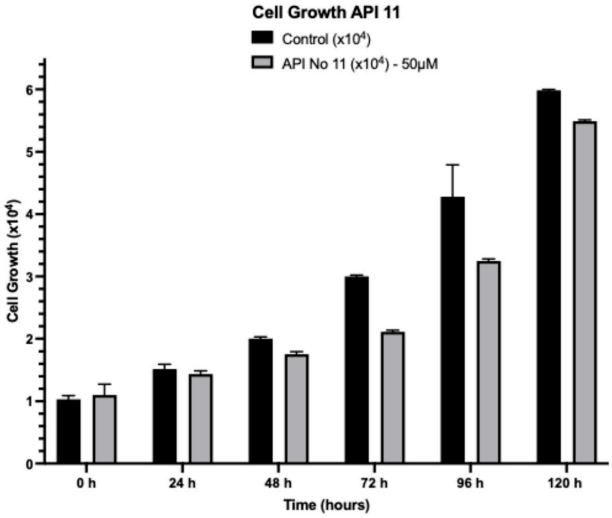
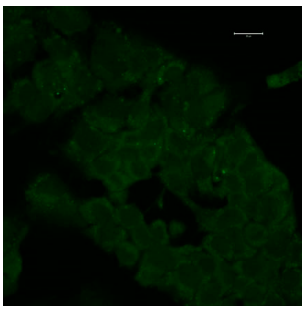
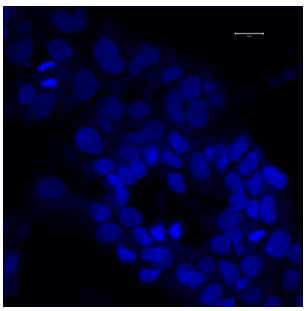
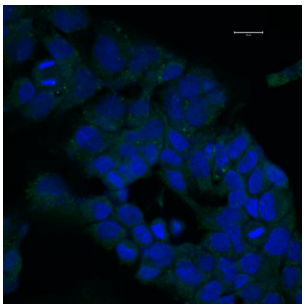
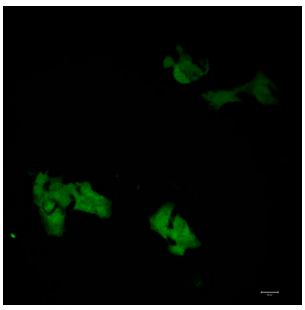
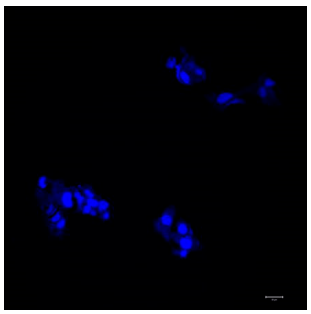
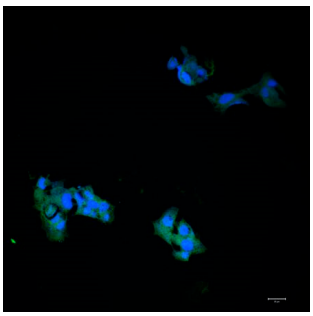


Figure 7. Cell growth and death assessment (24–120 h) of HepG2 cells exposed to treatment with Custom Mixture, as measured with the Neubauer counting chamber. The data present statistically significant differences ($p < 0.05$) compared to different treatments (n = 3).

Table 4. Group of confocal images of HepG2 cells exposed to treatment of Custom Mixture, as measured with the proliferation marker Ki-67.

	KI-67	DAPI	MERGED
Control			
Custom Mixture			

qPCR analysis was used to gain molecular insights into the activity of the Custom Mixture. Several genes related to DNA repair and immune modulation, including ATM and XRCC1, were upregulated, suggesting potential protective genomic effects. Yet, these gene expression levels were lower than specific ones seen for certain individual APIs, indicative of a compromised DNA repair response. Similarly, the mixture was found to upregulate inflammatory markers like TNF, suggesting mild pro-inflammatory activity that could mediate its cytotoxic potential. These results show that the Custom Mixture can upregulate protective pathways while downregulating stress response pathways, indicating that its cellular effects are nuanced and multifactorial.

The Custom Mixture also produced a distinct gene expression profile compared with the individual APIs, with differences in the magnitude of fold regulation across several molecular targets. These findings indicate that the combined formulation modifies the molecular response observed with the individual constituents. Genes involved in DNA repair, like ATM and APEX1, were also highly upregulated. Reactive oxygen species and neurogenesis-related markers were moderately elevated (SIRT1; TREM2), implying enhanced stress responses and putative neuroprotective roles. For example, proliferation-related markers such as TNF were significantly overexpressed, along with inflammatory markers such as IL6 that were barely downregulated, indicating a pro-survival and anti-inflammatory balance. For drug metabolism pathways, CYP3A4 and ABCC2 increased significantly, suggesting enhanced metabolizing capacity. Importantly, the "Custom Mixture" results from a complex interplay between its components, providing moderate cell growth, some proliferation activity, and low-level apoptosis. Effects are shown in confocal images for both proliferation and apoptosis markers, and qPCR data further emphasize its subtle modulation of genomic stability and immune responses. The Combined Mixture may, therefore, hold therapeutic potential in the context of requiring a more balanced proliferative and cytostatic effect, although additional work and further exploration are needed to mitigate its pro-inflammatory tendencies and optimize its clinical benefits.

3.5. Targeted Real-Time qPCR Analysis in HepG2 Cells and Dendritic PBMCs Exposed in Custom Mixture of APIs 1–8

Both fold-up and fold-down regulation variabilities exhibited the significance of gene expression analysis differences on PBMCs and HepG2 cell lines. As in PBMCs, the Custom Mixture regulates a notable number of genes, including 107 upregulated and 79 downregulated genes, indicating that the Custom Mixture may impact a broad spectrum of cellular activity at the transcript level.

The fold-up regulation in PBMCs suggests it activates a particularly strong response, as measured by genes involved in DNA repair, stress response, and metabolic processes. An example is the gene XRCC1, which showed a high expression value when treated with the Custom Mixture, suggesting a relevant role in DNA damage repair mechanisms. Likewise, ATM increases, indicating the Custom Mixture could potentiate cellular stress responses. A previously noted regulation with APEX1 suggests its involvement in oxidative stress responses and DNA repair. BDNF was also significantly upregulated, which likely contributed to neuroprotection; CYP3A4 was upregulated moderately, suggesting an influence on drug metabolism pathways within PBMCs. The upregulation of these processes highlights a complex but strong cellular response to the Custom Mixture, specifically related to oxidative stress, DNA damage, and metabolic processes.

Conversely, multiple genes appeared to demonstrate fold-down regulation when subjected to the treatment of the Custom Mixture, potentially implicating some modulation of inflammatory and neurotrophic pathways. Interestingly, NTRK2 had one of the lowest values, suggesting that the signaling pathway is inhibited since neurotrophins are essential for the growth and survival of neurons. DCX, which was downregulated, suggested an inhibition of neuronal differentiation processes. The Custom Mixture potentially impacts homeostasis and SIRT1 with a pronounced downregulation. The Custom Mixture led to downregulation of IL1B and IL6 genes, which are known to cause inflammation, further indicating an anti-inflammatory effect (Figure 8). These downregulated pathways imply that the Custom Mixture may inhibit inflammatory responses and neuronal signaling, counterbalancing its upregulated stress response gene by inhibiting inflammatory pathways.

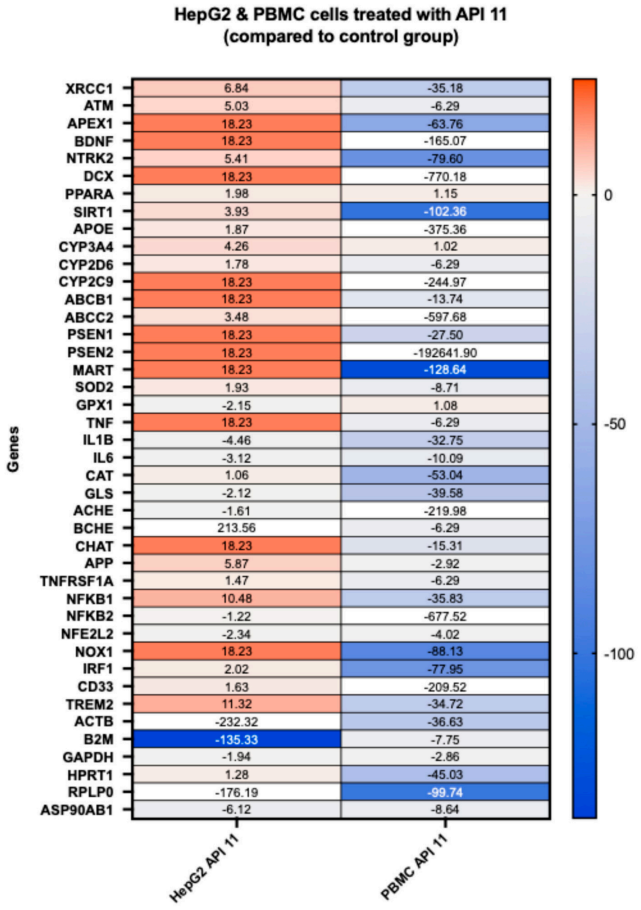


Figure 8. Heatmap representing the differentially expressed genes of HepG2 cells in comparison with PBMCs upon treatment with Custom Mixture compared with untreated control samples. Red color indicates the upregulated genes and blue the downregulated genes. The intensity of the color highlights the strength of the regulation.

In HepG2 cells, the Custom Mixture resulted in modestly altered gene expression but still revealed some interesting trends. Downregulation of SIRT1 at −1.16 indicated a slight inhibition of metabolic processes, while TNF and TNFRSF1A showed minor fluctuations, suggesting possible interactions with immune response pathways. HepG2 cells exhibit these changes, supporting a weaker effect, as compared to PBMCs, but are still indicative of beneficial metabolic and immune modulatory activities of the Custom Mixture.

3.6. Affected Molecular Pathways Analysis

The qPCR results revealed significant insights into the molecular profiles modulated by the olive oil constituents across API 1–8 and Custom Mixture in HepG2 cells and PBMCs (Figures 9–11). Many of the most active APIs, such as oleocanthal (API 1) and hydroxytyrosol (API 7) exhibited rigorous upregulation of genes that play a key role in DNA repair and cell cycle regulation, notably of XRCC1, ATM, and APEX1, in the HepG2 cells. These genes are involved in the maintenance of genomic stability, which indicates that these APIs may protect against genotoxic stress and aid cancer cell survival by relevant mechanisms of DNA repair. Similarly, the Custom Mixture modulated DNA repair-associated pathways in HepG2 cells, although the magnitude of this response differed from that observed with the individual compounds. In contrast, DNA repair genes were predominantly downregulated in PBMCs. This divergence demonstrates distinct regulation of DNA repair-associated genes between HepG2- and PBMC-derived dendritic cells, indicating a cell-type-dependent

transcriptional response to the Custom Mixture. Such modulation may help dampen excessive immune responses and protect against immune cell overactivation.

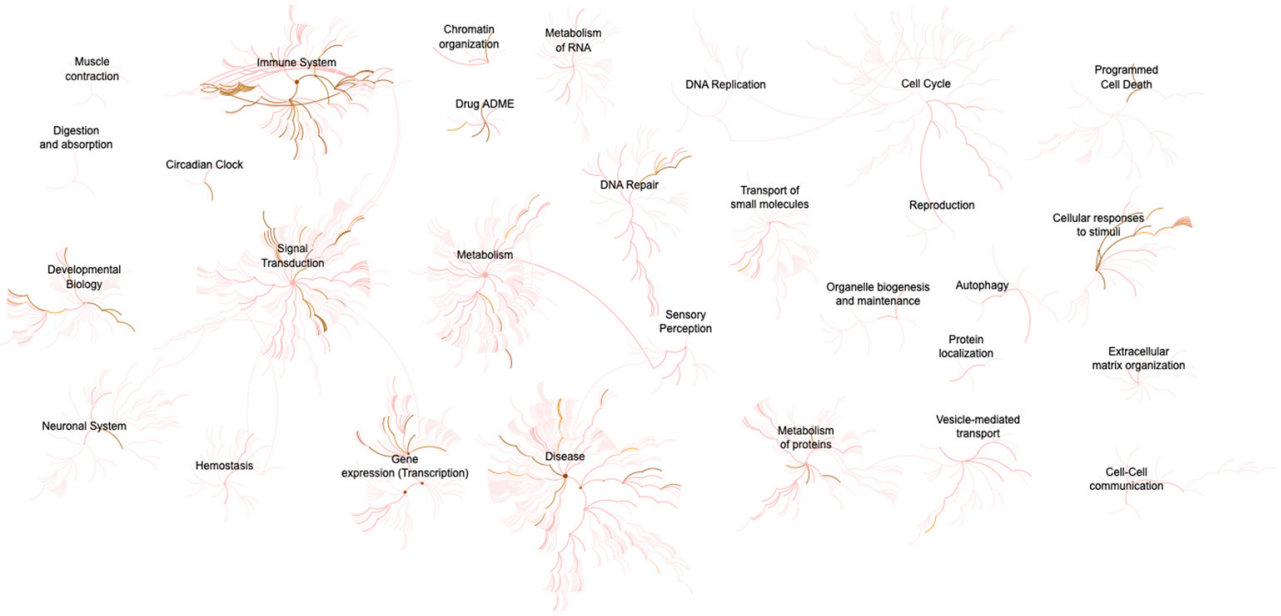


Figure 9. Genome-wide overview of the results of pathway analysis. Reactome pathways are arranged in a hierarchy. The center of each of the circular "bursts" is the root of one top-level pathway. Each step away from the center represents the next level lower in the pathway hierarchy. The color code denotes over-representation of that pathway in dataset. Light grey signifies pathways which are not significantly over-represented.

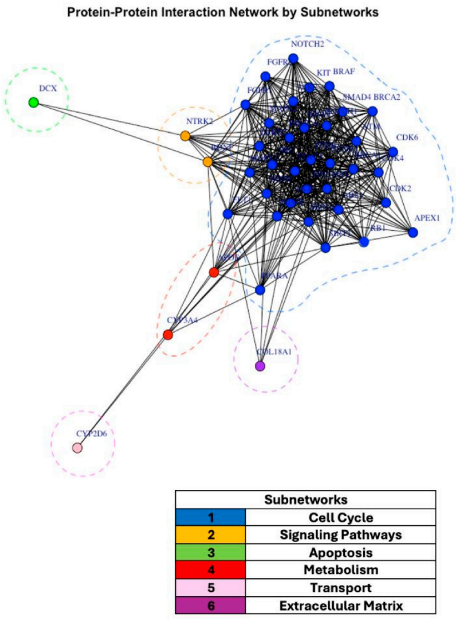


Figure 10. PPI network. PPI network showing the interactions amongst the proteins identified in HepG2 cells. The network was constructed using the STRING-DB tool. The proteins are shown with different colors depending on the subnetwork they belong to. The line width indicates the confidence in data support. A minimum confidence interaction of 0.8 was selected for high confidence. The multi-colored dotted lines enclose 6 different subnetworks of proteins.

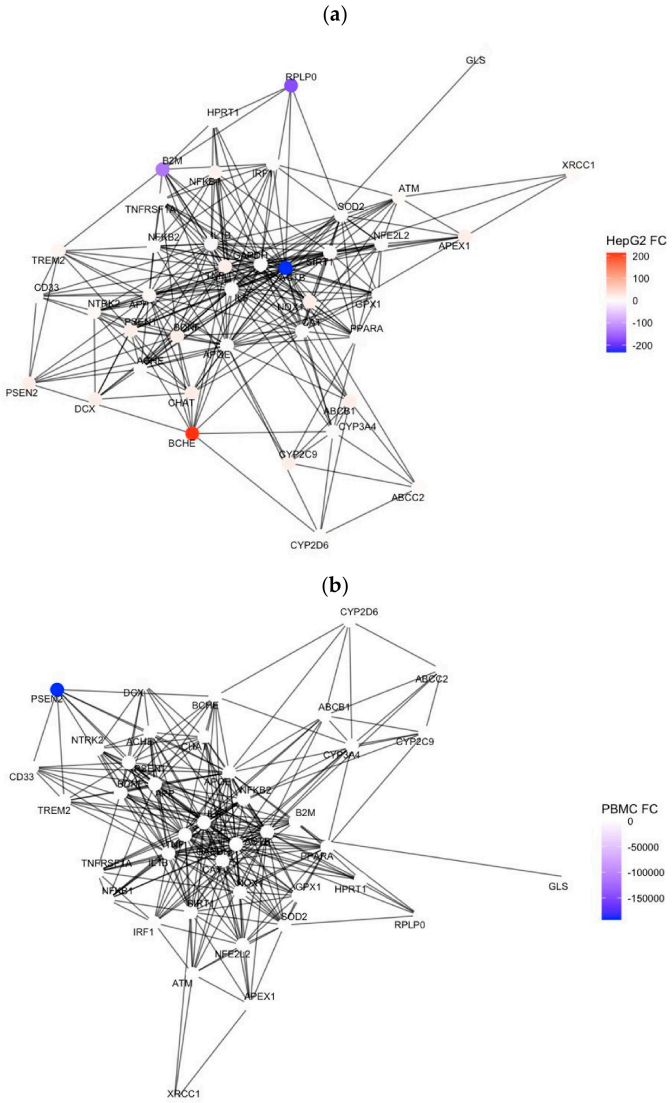


Figure 11. Protein–protein interaction (PPI) network for Custom Mixture comparison between HepG2 cells and PBMCs. (**a**) This network visualizes predicted protein–protein interactions among the genes regulated by the specified API in HepG2 cells, while (**b**) visualizes predicted protein–protein interactions among the genes regulated in PBMCs. Nodes represent gene-encoded proteins, and edges indicate known or predicted functional associations from the STRING database. Node color reflects the magnitude and direction of fold regulation, with upregulated genes in red, downregulated genes in blue, and white indicating no change.

Neurotrophic signaling and metabolic regulation pathways were also significantly enriched across APIs, with the most pronounced difference between the responses of HepG2 cells and PBMCs. A second mechanism involved the upregulation of several neurotrophic genes (e.g., BDNF and NTRK2), which were consistently upregulated in the HepG2 cells treated with certain APIs (particularly Custom Mixture), suggesting that APIs could enhance cell survival, or that cell protection could take place (potentially neuroprotective) in this model of liver cancer. This upregulation may indicate enhanced cell resilience and metabolic capacity to support growth, potentially promoting HepG2 proliferation. These same genes were strongly downregulated by the Custom Mixture in PBMCs, suggesting a cell-type-specific metabolic suppression that may have the potential to reduce inflammation- and oxidative stress-related gene expression and pathway-level responses. The mixture acts as a growth and trophic support factor in cancer cells but as

an inhibitor of these pathways in immune cells, indicating a potential immune-permissive environment via limitation of immune cell activation and energy consumption.

Additionally, metabolism-related characterization and differential models of lipid metabolism and energy homeostasis genes (e.g., APOE, PPARA) highlighted the heterogeneous responses observed between HepG2 cells and PBMCs. APIs 1 and 7 mildly upregulated APOE and PPARA in HepG2 cells, consistent with their supporting cellular growth and lipid metabolism. This improvement is in line with the positive proliferative impacts in the HepG2 cells, and it suggests that these APIs may further aid in the production of energy and lipids needed by cells to allow for the metabolic demands of actively proliferating cells. The downregulation of these genes by Custom Mixture treatment may represent a metabolic restraint mechanism that attenuates the activity of immune cells, such as limiting cellular energy use and lipid metabolism. This metabolic suppression may help reduce inflammation and energy consumption in PBMCs, which are associated with numerous APIs' antioxidant and anti-inflammatory effects.

Finally, pathways related to immune signaling and oxidative stress demonstrated complex, cell-specific regulation, where Custom Mixture treatment moderately downregulated pro-inflammatory genes such as IL1B and IL6 in HepG2 cells and PBMCs. This anti-inflammatory action is more pronounced in PBMCs, where it modulates immune activation. On the other hand, in HepG2 cells, the response is more regulated. Genes related to antioxidant defense, including SOD2 and GPX1, were also oppositely regulated, with upregulation in HepG2 cells and downregulation in PBMCs with mixture treatment. These results indicate that the Custom Mixture can increase antioxidant potential in a homogenous manner in HepG2 cells, which may protect cancer cells from cellular death due to oxidative stress. At the same time, it reduces oxidative stress in PBMCs, which in turn may contribute to the decrease in immune cell activation level and inflammation that is associated with it. Collectively, these findings demonstrate distinct transcriptional responses to the Custom Mixture in HepG2- and PBMC-derived dendritic cells, emphasizing the influence of cellular context on the molecular response to the investigated olive oil constituents.

4. Discussion

4.1. Proliferation, Cytotoxicity, and Time-Dependent Effects

Among the tested compounds, API 1 (oleocanthal) and API 7 (hydroxytyrosol) consistently exhibited a medium rate of cell toxicity in HepG2 cells. This was evidenced by the moderate levels of cell viability at multiple time points, as the concentration increased, reaching a viability of 65–70%, which is observed especially in API 1. These findings align with previous reports showing that hydroxytyrosol significantly inhibits HepG2 proliferation at concentrations ranging from 10 to 100 μM [51], and that oleocanthal suppresses cell proliferation and survival in liver cancer models at 10–20 μM in vitro [25]. Additional studies have demonstrated that oleocanthal decreases viability in hepatocellular carcinoma cells, including HepG2 and Hep3B, at 10–50 μM [52,53], supporting the moderate cytotoxicity observed in the present work. Confocal microscopy further supported these effects, visually confirming moderately preserved nuclear integrity and cellular morphology in cells treated with APIs 1 and 7. These treatments were associated with moderate to high mitosis rates and limited apoptotic features, indicating controlled cell cycle progression.

In contrast, API 4 (oleuropein aglycon), API 5 (oleomissional), and API 6 (tyrosol) induced significant cytotoxic effects. These compounds reduced cell viability and mitosis across all conditions and triggered classical apoptotic features, including chromatin condensation and nuclear fragmentation, as observed in confocal microscopy. These findings are consistent with earlier studies showing that tyrosol exerts pro-apoptotic effects in liver

cancer cells at 25–100 μM, reducing viability and activating mitochondrial apoptotic pathways [50,54]. These outcomes were further substantiated by gene expression data showing downregulation of antioxidant genes (e.g., CAT, IL6) and upregulation of inflammatory cytokines such as TNF, which are known to mediate stress-induced apoptosis. Recent studies demonstrated tyrosol-induced mitophagy and apoptotic signaling in liver cancer cells, confirming the cytotoxic effects observed with API 6 treatment [55,56]. Oleuropein aglycon's cytotoxicity is also well documented; its lipophilic structure promotes mitochondrial accumulation, altering membrane fluidity and increasing RS production, leading to apoptosis at 20–100 μM in HepG2 and other cancer cell lines [11,57]. These mechanistic insights align with the strong cytotoxic profile of API 4 in the present study.

Time course analysis revealed that APIs 1 and 7 maintained moderate cellular viability even at 96 h of exposure. In contrast, APIs 4, 5, and 6 caused progressive reduction in cell viability over the period of 72 h in culture, suggesting time-dependent cytotoxicity effects. This pattern likely reflects a combination of adaptive cellular responses, including the survival and proliferation of more resistant cell subpopulations, activation of cytoprotective mechanisms, and metabolic adaptation following the initial cytotoxic insult.

Taken together, these findings demonstrate that the individual phenolic compounds produce distinct cellular response profiles, ranging from relatively preserved viability and proliferative activity to more pronounced cytotoxic effects. Establishing these individual profiles was essential for the principal objective of the study, namely the evaluation of their combined effects within the Custom Mixture. The individual compounds therefore provide the experimental reference against which the biological behavior of the mixture can be interpreted, allowing us to assess whether combining the phenolics reproduces, enhances, attenuates, or modifies their individual effects.

The Custom Mixture demonstrated a balanced biological profile regarding cell proliferation since mild cytotoxicity effects were observed. While the Custom Mixture modestly increased cell viability, this does not coincide with the increased cell proliferation rate as measured by cell growth and the Ki-67 proliferation marker. Such results for the Custom Mixture highlight its potential utility in applications requiring regulated cell growth interventions, including tissue repair or immune modulation activities. Notably, the mixture produced a sustained effect over time, maintaining stable viability up to 120 h. This prolonged activity contrasts with the time-limited cytotoxicity of APIs 4–6 and the peak viability of APIs 1 and 7 at 96 h.

The time-dependent stability of the Custom Mixture is further supported by similar work, which showed that olive polyphenols can modulate viability over extended periods and maintain controlled growth [55]. Similarly, multi-component polyphenol formulations enhance therapeutic efficacy through synergy and reduce toxicity, consistent with our observation of long-term viability without excessive cytotoxicity [58]. The Custom Mixture's time-dependent and balanced effects underscore its therapeutic potential, particularly in chronic treatment scenarios requiring controlled proliferation and low toxicity. These findings reinforce the value of polyphenol combinations in cancer chemoprevention and regenerative medicine and highlight the importance of time course studies to understand their biological impact.

While these cellular endpoints demonstrate clear differences between the individual phenolics and the Custom Mixture, measurements of viability and proliferation alone cannot explain the molecular mechanisms underlying these responses. We therefore extended the comparison to gene expression and pathway-level analyses. This enabled us to determine whether the distinct cellular phenotypes observed after treatment were accompanied by corresponding changes in molecular pathways involved in DNA repair, oxidative stress, inflammation, neurotrophic signaling, and cell cycle regulation.

4.2. Molecular Effects of Olive Oil Polyphenols: Pathway-Oriented Insights in HepG2 Cells and PBMCs

The molecular analysis revealed that the biological effects of olive oil phenolics cannot be explained by the modulation of a single molecular target or pathway. Instead, the treatments produced distinct but interconnected changes across several cellular processes. To provide a clearer interpretation of these findings, the following sections discuss the principal molecular responses according to their functional context, beginning with DNA damage and repair and subsequently considering oxidative stress, inflammatory signaling, neurotrophic responses, and cell cycle regulation. Particular attention is given to whether the Custom Mixture reproduces or modifies the molecular responses observed with its individual constituents.

4.2.1. DNA Damage Response and Repair: ATM and XRCC1 Activation

DNA repair is essential for preserving genomic integrity, particularly in cancer, where genomic instability drives tumorigenesis. In this RT-qPCR analysis, significant upregulation of ATM and XRCC1 was observed in HepG2 cells treated with API 1 (oleocanthal) and API 7 (hydroxytyrosol). ATM is a master regulator of the DNA damage response, particularly in detecting and repairing double-strand breaks (DSBs), initiating downstream phosphorylation cascades affecting p53, H2AX, and BRCA1 [59]. In parallel, XRCC1 is integral to the base excision repair (BER) pathway and single-strand break repair (SSBR), functioning as a scaffold protein that recruits DNA ligase III and PARP1 to repair oxidized bases and strand breaks [60]. These gene expression patterns suggest that specific olive oil polyphenols can significantly enhance the genomic surveillance machinery in liver cancer cells. Comparable activation of DNA repair pathways has been reported for hydroxytyrosol at 10–50 μM in hepatic and neuronal models, where it promotes genomic stability and neuroprotection [30].

Interestingly, the Custom Mixture, composed of several bioactive phenolics, elicited only a moderate increase in ATM and XRCC1 expression. This may indicate complex interactions—possibly antagonistic or regulatory—among polyphenols that tune the DNA repair response, preventing overactivation or excessive energy consumption under basal stress levels. In PBMCs, the induction of ATM and XRCC1 was less pronounced, seen mostly with hydroxytyrosol. However, even modest upregulation points to a conserved protective role in immune cells, which face regular oxidative and environmental challenges. This aligns with the role of ATM and XRCC1 in immune surveillance and DNA repair during inflammatory responses. Enrichment analysis further reinforced these observations, highlighting the activation of critical pathways such as homologous recombination, base excision repair, and p53-mediated DNA damage signaling under treatment with APIs 1 and 7. These pathways were notably suppressed in untreated controls and completely absent in pro-inflammatory treatments (APIs 5 and 6), suggesting that only certain polyphenols selectively engage DNA repair programs, a property valuable for chemoprevention and therapy.

4.2.2. Oxidative Stress Mitigation: Antioxidant Enzymes SOD2 and GPX1

RS are key oncogenic transformation and therapy resistance mediators, promoting DNA damage, lipid peroxidation, and altered redox signaling [61]. The results showed strong upregulation of antioxidant enzymes SOD2 and GPX1 in HepG2 cells treated with API 7 (hydroxytyrosol). SOD2 is a mitochondrial enzyme that converts superoxide radicals ($O_2\bullet^-$) into hydrogen peroxide (H_2O_2), while GPX1 detoxifies H_2O_2 and lipid peroxides by utilizing glutathione, thus preventing RS accumulation and mitochondrial dysfunction [62]. Hydroxytyrosol has been shown to preserve mitochondrial membrane potential

and enhance antioxidant defenses in hepatic cells at 10–100 μM [63], consistent with the present findings.

The Custom Mixture induced a more moderate antioxidant response, suggesting that polyphenol blends may create a finely tuned redox buffering effect, neither too strong to trigger compensatory ROS production nor too weak to leave cells vulnerable. This fits with the hormesis hypothesis of polyphenol action, where mild stress induced by antioxidants activates endogenous protective pathways without tipping into cytotoxicity. In PBMCs, SOD2 and GPX1 were upregulated, particularly by hydroxytyrosol and the Custom Mixture, with lower fold changes than in HepG2 cells. PBMCs often function under oxidative bursts during immune activation, so that this redox balancing may contribute to immune cell homeostasis and viability under stress conditions. Pathway enrichment data confirmed the activation of key redox signaling modules, including glutathione metabolism, RS detoxification, and the NRF2 antioxidant response. These pathways were especially prominent under API 7 treatment, underscoring their therapeutic relevance in cancer prevention and oxidative stress disorders.

4.2.3. Inflammatory Pathway Modulation: TNF, IL1B, and IL6

Chronic inflammation is a hallmark of cancer, contributing to DNA damage, immune evasion, and sustained proliferation. This analysis revealed that treatment with API 5 (oleomissional) and API 6 (tyrosol) significantly upregulated TNF expression in HepG2 cells, accompanied by moderate increases in IL1B and IL6. This pro-inflammatory signature was associated with confocal imaging evidence of apoptotic morphology, including nuclear condensation and fragmentation. These findings suggest that inflammation-mediated cytotoxicity may contribute to the antitumor action of some olive polyphenols. Olive-derived phenolics have been shown to modulate inflammatory cascades by regulating TNF-α and IL-1β levels in vitro at 10–50 μM [2], supporting the present observations. Thus, the pro-inflammatory phenotype observed may reflect a shift toward programmed cell death rather than pathological inflammation.

Conversely, API 7 (hydroxytyrosol) displayed a dual phenotype, moderately upregulating TNF and IL1B while strongly enhancing antioxidant defenses, indicating a context-dependent modulation of inflammation and oxidative stress. This duality is crucial for maintaining redox-inflammatory balance during cell stress responses. The Custom Mixture interestingly suppressed IL1B and IL6 expression in HepG2 cells and PBMCs, indicating an immune regulatory effect that limits chronic inflammation while preserving homeostatic immune signaling. Such modulation could be critical for reducing cancer-associated inflammation without compromising immune defense. In PBMCs, the inflammatory response was more evident under API 5 and 6, which elevated TNF and IL1B, potentially activating immune signaling cascades. This selective pro-inflammatory response may be beneficial in immuno-oncology contexts, where immune activation is required, yet could be problematic in chronic inflammatory conditions. Enrichment analysis confirmed activation of NF-κB signaling, cytokine–cytokine receptor interaction, and TNF-mediated apoptosis pathways in HepG2 cells treated with APIs 5 and 6. In contrast, NF-κB activity was downregulated or absent in treatments with Custom Mixture and API 7, supporting their anti-inflammatory or balanced regulatory roles.

4.2.4. Cell Cycle Regulation and Proliferation: APEX1 and BDNF

Proper cell cycle and proliferation regulation is a cornerstone of cancer therapy. HepG2 cells treated with API 1 (oleocanthal) and API 7 (hydroxytyrosol) showed strong upregulation of APEX1 and BDNF. APEX1 functions as a central coordinator of the base excision repair (BER) pathway and that of the cellular redox signaling, while BDNF is a neurotrophic

factor implicated in cell survival and neuroimmune crosstalk, also influencing PI3K/AKT and MAPK pathways [64,65]. This expression pattern reflects the controlled proliferation and survival phenotype, which may prevent unchecked mitosis and favor DNA repair before division. Confocal imaging supported this, showing moderate mitotic figures without signs of hyperproliferation, indicating a non-tumorigenic effect. Oleocanthal has been shown to induce G0/G1 arrest in liver cancer cells at 10–20 μM [25], supporting the present findings. Oleuropein aglycon (API 4) has also been reported to inhibit cell cycle progression via p21 and p27 induction at 20–50 μM [31], consistent with the reduced proliferative markers observed under API 4.

In PBMCs, APEX1 remained stable or slightly downregulated, while BDNF was modestly increased under hydroxytyrosol and Custom Mixture treatment. This may reflect a protective mechanism to preserve immune cell viability and neuroimmune communication under redox-modulating conditions, without inducing abnormal proliferation. Enrichment analysis revealed activation of cell cycle checkpoint pathways, particularly G1/S transition control, MAPK signaling, and p53–APEX1 regulatory axes in HepG2 cells treated with APIs 1, 7, and 10. These networks are vital for ensuring DNA repair before replication and reflect the balanced anti-cancer mechanism promoted by these polyphenols.

4.3. Cell-Type-Dependent Responses to the Custom Mixture in HepG2- and PBMC-Derived Dendritic Cells

The comparison between individual phenolics and the Custom Mixture provides one level of interpretation; however, the biological response to a complex phenolic formulation also depends on the cellular context in which it acts. To investigate this aspect, we further compared the molecular response to the Custom Mixture between HepG2 cells and PBMCs. This comparison revealed markedly different gene expression patterns, indicating that the effects of the combined phenolics are strongly influenced by cell-specific physiology and function.

HepG2 cells are cancer cells, and they have improved stress response capabilities to handle the DNA damage and oxidative stress caused by rapid cell division. This is evidenced by the upregulation of DNA repair genes, including XRCC1, ATM, and APEX1, essential for genomic stability and tumor progression. The Custom Mixture may amplify these pathways in HepG2 cells, contributing to cellular survival and resistance to oxidative stress. This is consistent with previous findings showing that olive phenolics activate DNA repair pathways in cancer cells at 10–50 μM [65]. Upregulation of neurotrophic and detoxification pathways further supports the enhanced survival capacity of HepG2 cells under stress [66].

PBMCs are considered biomarkers of immune dysfunction and provide insights into how olive oil polyphenols modulate their gene expression, which is an important starting point for their further implementation as markers of their beneficial effect on disease [66,67]. The pathophysiology of PBMCs, immune cells, differs significantly from that of cancer cells. PBMCs have lower baseline levels of DNA repair activity than cancer cells, as PBMCs are adapted for immune surveillance rather than rapid proliferation [68]. Analyses of PBMCs treated with the Custom Mixture revealed downregulation of DNA repair genes (XRCC1, APEX1, and BDNF), suggesting that the immune cells may be responding to the polyphenols in a way that curtails their ability to repair and proliferate. This downregulation is a counteraction to excessive activation and proliferation of these cell types due to oxidative stress or inflammatory cytokines, which can result in autoimmune reactions or chronic inflammatory and allergic diseases.

A second distinction is in line with the pathophysiology of immune cells, which need to balance activation and suppression to counteract potentially detrimental immune overactivation [69]. It suggests that immune cells may respond differently to two stimuli in an additive manner. The differential regulation of various DNA repair genes in peripheral

blood-like cells versus liver cells corroborates the notion that the Custom Mixture produces distinct transcriptional responses in HepG2 cells and PBMCs [70,71]. Hydroxytyrosol and related phenolics have been shown to modulate immune responses and reduce oxidative stress in PBMCs at 10–50 μM [12], consistent with the present findings. In principle, immune system elements are naturally inhibited from proliferative processes in the reaction to inflammation to prevent excessive immune activation, and the Custom Mixture's downregulation of DNA repair in PBMCs may represent a downregulatory mechanism intended to adjust immune activity and see excessive immune activation as undesirable.

The downregulation of neurotrophic and metabolic pathways in PBMCs also fits with the pathophysiology of immune cells, which typically have less need for the neurotrophic support necessary for cancer cells [72,73]. These results of suppression of BDNF and NTRK2 in PBMCs treated with the Custom Mixture could suggest the response of these cells to olive oil polyphenols by reducing the signaling pathways not required for their immune functions but instead needed by cancer cells for survival. The downregulation of genes associated with lipid metabolism and mitochondrial function also supports the idea that the Custom Mixture is blocking energy-expending processes in immune cells due to suppressing metabolic pathways in PBMCs. Such a response may act as a protective mechanism by lowering metabolic processes and conserving energy toward those functioning processes to avoid immune dysfunction. These effects in PBMCs likely reflect a proclivity towards a decrease in oxidative stress and inflammatory pathways that reduces the potential for autoimmune responses, but not so far as to predispose too aggressively towards inflammation or active immune activation.

Conversely, these pathways were upregulated in tumor cells such as HepG2, highlighting a feature that allows the cancer cells to survive and proliferate despite harsh environmental conditions. Moreover, the distinct gene expression profile of HepG2 cells as compared to PBMCs developing on induction with the Custom Mixture of olive oil polyphenols reflects the contribution of cell context-dependent pathophysiology to their responses. The Custom Mixture promotes DNA repair, neurotrophic signaling, and metabolic pathways, enhancing cancer cell survival and proliferation in HepG2 cells. PBMCs, however, show a downregulation of DNA repair and neurotrophic pathways, which is likely necessitated by the need of immune cells to downregulate excessive activation and proliferation to prevent autoimmune responses and chronic inflammation [74].

An important limitation of the present study is the predominant use of the HepG2 hepatocellular carcinoma cell line. Although HepG2 cells are a well-established model for investigating hepatic cellular and molecular responses, their cancer-derived phenotype and metabolic characteristics do not fully represent those of normal human hepatocytes. Moreover, the concentrations and exposure conditions used in vitro should not be considered directly equivalent to those achieved following dietary EVOO consumption. Therefore, the present findings should primarily be interpreted as mechanistic evidence of the responses to selected olive oil minor constituents under controlled experimental conditions. As a non-malignant hepatic model was not included, the observed differences cannot establish tumor selectivity. Further studies using primary human hepatocytes or other non-transformed hepatic models, followed by appropriate in vivo studies, are required to determine the physiological relevance and potential selectivity of these effects.

5. Conclusions

The present study provides an integrated evaluation of the biological and molecular effects of selected EVOO phenolic compounds, with particular emphasis on understanding how their individual activities relate to the response produced when they are combined in a representative Custom Mixture. Although several of these phenolics have previously

been investigated individually, their evaluation in the present study provided the necessary experimental reference for interpreting the behavior of the combined formulation.

The individual phenolics produced distinct cellular and molecular profiles in HepG2 cells. Differences were observed in cell viability, proliferation, and the regulation of pathways associated with DNA repair, oxidative stress, inflammation, neurotrophic signaling, metabolism, and cell cycle control. These compound-specific responses established that structurally related olive oil phenolics do not necessarily produce equivalent biological effects under the same experimental conditions.

Importantly, the Custom Mixture did not simply reproduce the activity of any single constituent or uniformly amplify the responses observed with the individual compounds. Instead, it exhibited a more integrated biological profile, characterized by relatively stable viability over prolonged exposure and coordinated modulation of multiple molecular pathways. The differences between the individual and combined treatments suggest that interactions among phenolic constituents may modify their biological activity when present together. These interactions may include additive, regulatory, synergistic, or antagonistic components and require further investigation to define their individual contributions.

A further level of complexity was demonstrated by the comparison between HepG2 cells and PBMCs. The Custom Mixture produced distinct gene expression responses in the two cellular systems, particularly in pathways associated with DNA repair, oxidative stress, neurotrophic signaling, metabolism, and immune regulation. These findings indicate that the molecular response to combined olive oil phenolics is not only dependent on mixture composition but also strongly influenced by cellular context.

Taken together, the study supports a narrative in which the biological effects of EVOO phenolics progress from compound-specific activities to more complex responses when the constituents are combined, with the final molecular outcome being further shaped by the cellular environment. Thus, the principal contribution of this work lies not in attributing the effects of olive oil to a single phenolic compound but in providing a comparative framework for understanding how individual phenolic activities are modified within a complex mixture. This approach may contribute to a more mechanistic understanding of the biological activity of phenolic-rich olive oil, while further studies are required to characterize the interactions among individual constituents and to establish their relevance in more physiologically representative models.

Supplementary Materials: The following supporting information can be downloaded at: https://www.mdpi.com/article/10.3390/futurepharmacol6040060/s1, Table S1: Microscopy Images of HepG2 Cell Growth and Death Following Treatment with APIs 1–8 & Custom mixture (API 11) (24–120 h); Table S2: Microscopy Images of HepG2 Cell Toxicity Following Treatment with APIs 1–8 & Custom Mixture (API 11) (24–120 h); Table S3: Cell structure images of HepG2 cells exposed to various treatments of APIs 1-8, as measured with Phase Contrast Microscope; Table S4a: Real-Time qPCR results of HepG2 cells Following Treatment with APIs 1–8. Down-Regulated genes highlighted with blue and Up-Regulated genes highlighted with red; Table S4b: Real-Time qPCR results of HepG2 cells Following Treatment with APIs 1–8. Down-Regulated genes highlighted with blue and Up-Regulated genes highlighted with red; Table S5: Compared Analysis of Real-Time qPCR results of HepG2 cells Treated with APIs 1–8 vs API 11. Down-Regulated genes highlighted with blue and Up-Regulated genes highlighted with red; Table S6: Real-Time qPCR results of HepG2 & PBMC cells Following Treatment with API 11. Down-Regulated genes high-lighted with blue and Up-Regulated genes highlighted with red.

Author Contributions: S.I.P.: writing—original draft, conceptualization, methodology, project administration, methodology, formal analysis, validation, and visualization; F.C.: writing—review and editing, data curation, and validation; L.K.: writing—review and editing, formal analysis, and visualization; E.K.: writing—review and editing, and formal analysis; P.M.: writing—review and editing, and resources; V.V.: writing—review and editing, resources, supervision, project administration, and methodology; I.S.V.: writing—review and editing, resources, conceptualization, supervision, project administration, and methodology. All authors have read and agreed to the published version of the manuscript.

Funding: This research was funded by the interdepartmental public funds of Aristotle University of Thessaloniki (ELKE Auth-5596), School of Public Health—Yale University and the company Yanni's Olive Grove.

Institutional Review Board Statement: Not applicable.

Informed Consent Statement: Not applicable.

Data Availability Statement: The data presented in this study are available on request from the corresponding author as this research was part of a company's project.

Acknowledgments: We would like to thank Prokopios Magiatis for its generous supply of the tested olive oil isolated constituents and the company Yanni's Olive Grove for its financial support. The authors would also like to thank Emmanuel Panteris (School of Biology, Aristotle University of Thessaloniki, Greece) for his help with the confocal microscopy experiments. During the preparation of this manuscript, the authors used ChatGPT (OpenAI, GPT-6, October 2026) and its image generation capabilities for the creation and visual refinement of the graphical abstract. The prompts instructed the tool to generate a scientific graphical abstract illustrating the investigation of isolated olive oil phenolic compounds and their Custom Mixture, including the HepG2 and peripheral immune cell experimental models, the evaluated molecular pathways, and the principal findings. The authors reviewed and edited the generated output and take full responsibility for the accuracy, integrity, and content of the graphical abstract and the publication.

Conflicts of Interest: The authors declare no conflicts of interest. Sofia I. Prodromou has received sponsorship for her Ph.D. research project from the company "Yanni's Olive Grove". The funders had no role in the design of the study; in the collection, analyses, or interpretation of data; in the writing of the manuscript; or in the decision to publish the results.

Abbreviations

The following abbreviations are used in this manuscript:

ABCB1	ATP-Binding Cassette Subfamily B Member 1
ABCC2	ATP-Binding Cassette Subfamily C Member 2
ACHE	Acetylcholinesterase
ACTB	Beta-Actin
APEX1	Apurinic/Apyrimidinic Endodeoxyribonuclease 1
API	Active Pharmaceutical Ingredient
APOE	Apolipoprotein E
APP	Amyloid Precursor Protein
ATM	Ataxia-Telangiectasia Mutated Protein
B2M	Beta-2-Microglobulin
BCHE	Butyrylcholinesterase
BDNF	Brain-Derived Neurotrophic Factor
CAT	Catalase
CD33	Myeloid Cell Surface Antigen CD33
CHAT	Choline O-Acetyltransferase

COX	Cyclooxygenase
CREB	cAMP Response Element-Binding Protein
CYP2C9	Cytochrome P450 2C9
CYP2D6	Cytochrome P450 2D6
CYP3A4	Cytochrome P450 3A4
DCX	Doublecortin
DLC	Dual Label Confocal
EVOO	Extra Virgin Olive Oil
GAPDH	Glyceraldehyde-3-Phosphate Dehydrogenase
GPX1	Glutathione Peroxidase 1
HepG2	Human Hepatocellular Carcinoma Cell Line
HPRT1	Hypoxanthine Phosphoribosyltransferase 1
IL1B	Interleukin 1 Beta
IL6	Interleukin 6
IRF1	Interferon Regulatory Factor 1
NFE2L2	Nuclear Factor Erythroid 2-Related Factor 2
NFKB1	Nuclear Factor Kappa B Subunit 1
NFKB2	Nuclear Factor Kappa B Subunit 2
NOX1	NADPH Oxidase 1
NSAID	Non-Steroidal Anti-Inflammatory Drug
NTRK2	Neurotrophic Receptor Tyrosine Kinase 2
PBMC	Peripheral Blood Mononuclear Cell
PPARA	Peroxisome Proliferator-Activated Receptor Alpha
PSEN1	Presenilin 1
PSEN2	Presenilin 2
ROS	Reactive Oxygen Species
RPLP0	Ribosomal Protein Lateral Stalk Subunit P0
SIRT1	Sirtuin 1
SOD2	Superoxide Dismutase 2
TNF	Tumor Necrosis Factor
TNFRSF1A	TNF Receptor Superfamily Member 1A
TREM2	Triggering Receptor Expressed on Myeloid Cells 2
XRCC1	X-ray Repair Cross Complementing Protein 1

References

1. Guasch-Ferré, M.; Willett, W. The Mediterranean diet and health: A comprehensive overview. *J. Intern. Med.* **2021**, *290*, 549–566. [CrossRef] [PubMed]
2. Bucciantini, M.; Leri, M.; Nardiello, P.; Casamenti, F.; Stefani, M. Olive polyphenols: Antioxidant and anti-inflammatory properties. *Antioxidants* **2021**, *10*, 1044. [CrossRef] [PubMed]
3. Jimenez-Lopez, C.; Carpena, M.; Lourenço-Lopes, C.; Gallardo-Gomez, M.; Lorenzo, J.M.; Barba, F.J.; Prieto, M.A.; Simal-Gandara, J. Bioactive compounds and quality of extra virgin olive oil. *Foods* **2020**, *9*, 1014. [CrossRef] [PubMed]
4. Singh, R.B.; Watson, R.R.; Takahashi, T. *The Role of Functional Food Security in Global Health*; Academic Press: Cambridge, MA, USA, 2019; pp. 623–637. [CrossRef]
5. Abuznait, A.H.; Qosa, H.; Busnena, B.A.; El Sayed, K.A.; Kaddoumi, A. Olive-oil-derived oleocanthal enhances β-amyloid clearance as a potential neuroprotective mechanism against Alzheimer's disease disease: In vitro and in vivo studies. *ACS Chem. Neurosci.* **2013**, *4*, 973–982. [CrossRef] [PubMed]
6. Romani, A.; Ieri, F.; Urciuoli, S.; Noce, A.; Marrone, G.; Nediani, C.; Bernini, R. Health effects of phenolic compounds found in extra-virgin Olive Oil, By-Products, and Leaf of *Olea europaea* L. *Nutrients* **2019**, *11*, 1776. [CrossRef] [PubMed]
7. Mileo, A.M.; Miccadei, S. Polyphenols as Modulator of Oxidative Stress in Cancer Disease: New Therapeutic Strategies. *Oxid. Med. Cell. Longev.* **2016**, *2016*, 6475624. [CrossRef] [PubMed]
8. Pérez-Jiménez, F.; Ruano, J.; Perez-Martinez, P.; Lopez-Segura, F.; Lopez-Miranda, J. The influence of olive oil on human health: Not a question of fat alone. *Mol. Nutr. Food Res.* **2007**, *51*, 1199–1208. [CrossRef] [PubMed]
9. Rafehi, H.; Ververis, K.; Karagiannis, T.C. Mechanisms of action of phenolic compounds in olive. *J. Diet. Suppl.* **2012**, *9*, 96–109. [CrossRef] [PubMed]

10. D'Archivio, M.; Santangelo, C.; Silenzi, A.; Scazzocchio, B.; Varì, R.; Masella, R. Dietary EVOO polyphenols and gut microbiota interaction: Are There Any Sex/Gender Influences? *Antioxidants* **2022**, *11*, 1744. [CrossRef] [PubMed]
11. Kahraman, G.; Özkaya, M.T.; Yıldırım, Ö. Potential anti-cancer effects of extra virgin olive oil and Its Phenolic Extracts on hepatocellular carcinoma cells. *Int. J. Nat. Life Sci.* **2023**, *7*, 112–122. [CrossRef]
12. Zorić, N.; Kopjar, N.; Rodríguez, J.; Tomić, S.; Kosalec, I. Protective effects of olive oil phenolics oleuropein and hydroxytyrosol against hydrogen peroxide-induced DNA damage in human peripheral lymphocytes. *Acta Pharm.* **2020**, *71*, 131–141. [CrossRef] [PubMed]
13. Xia, M.; Zhong, Y.; Peng, Y.; Qian, C. Olive Oil Consumption and Risk of Cardiovascular Disease and all-cause mortality: A meta-analysis of Prospective Cohort Studies. *Front. Nutr.* **2022**, *9*, 1041203. [CrossRef] [PubMed]
14. Serreli, G.; Deiana, M. Extra Virgin Olive Oil Polyphenols: Modulation of Cellular Pathways Related to Oxidant Species and Inflammation in Aging. *Cells* **2020**, *9*, 478. [CrossRef] [PubMed]
15. George, E.S.; Marshall, S.; Mayr, H.L.; Trakman, G.L.; Tatucu-Babet, O.A.; Lassemillante, A.-C.M.; Bramley, A.; Reddy, A.J.; Forsyth, A.; Tierney, A.C.; et al. The effect of high-polyphenol extra virgin olive oil on cardiovascular risk factors: A systematic review and meta-analysis. *Crit. Rev. Food Sci. Nutr.* **2019**, *59*, 2772–2795. [CrossRef] [PubMed]
16. Krenek, A.; Mathews, A.; Guo, J.; Courville, A.; Pepine, C.; Chung, S.; Aggarwal, M. Recipe for heart health: A randomized crossover trial on cardiometabolic effects of extra virgin olive oil within a whole-food plant-based vegan diet. *J. Am. Heart Assoc.* **2024**, *13*, e035034. [CrossRef] [PubMed]
17. Storniolo, C.E.; Casillas, R.; Bulló, M.; Castañer, O.; Ros, E.; Sáez, G.; Toledo, E.; Estruch, R.; Ruíz-Gutiérrez, V.; Fitó, M.; et al. Mediterranean diet supplemented with extra virgin olive oil or nuts improves endothelial markers involved in blood pressure control in hypertensive women. *Eur. J. Nutr.* **2015**, *56*, 89–97. [CrossRef] [PubMed]
18. Turck, D.; Bohn, T.; Cámara, M.; Castenmiller, J.; de Henauw, S.; Hirsch-Ernst, K.I.; Jos, A.; Maciuk, A.; Mangelsdorf, I.; McNulty, B.; et al. Phenolic compounds naturally present in olive oil and lowering of blood LDL-cholesterol and systolic blood pressure, therefore reducing the risk of coronary heart disease: Evaluation of a health claim pursuant to Article 14 of Regulation (EC) No 1924/2006. *EFSA J.* **2025**, *23*, 9470. [CrossRef] [PubMed]
19. Lucas, L.; Russell, A.; Keast, R. Molecular mechanisms of inflammation: Anti-inflammatory benefits of virgin olive oil and and the phenolic compound oleocanthal. *Curr. Pharm. Des.* **2011**, *17*, 754–762. [CrossRef] [PubMed]
20. Cicerale, S.; Keast, R. Oleocanthal, a natural anti-inflammatory compound in extra virgin olive oil. *Curr. Pharm. Des.* **2010**, *16*, 437–448. [CrossRef]
21. Butt, M.S.; Tariq, U.; Naz, A.; Rizwan, M. Neuroprotective effects of oleuropein: Recent developments and contemporary research. *J. Food Biochem.* **2021**, *45*, e13967. [CrossRef] [PubMed]
22. González-Rodríguez, M.; Ait Edjoudi, D.; Cordero-Barreal, A.; Farrag, M.; Varela-García, M.; Torrijos-Pulpón, C.; Ruiz-Fernández, C.; Capuozzo, M.; Lago, F.; Pino, J.; et al. Oleocanthal, an Antioxidant Phenolic Compound in Extra Virgin Olive Oil (EVOO): A Comprehensive Systematic Review of Its Potential in Inflammation and Cancer. *Antioxidants* **2023**, *12*, 2112. [CrossRef] [PubMed]
23. Goren, L.; Zhang, G.; Kaushik, S.; Breslin, P.A.S.; Du, Y.; Foster, D.A. (-)-Oleocanthal and (-)-oleocanthal-rich olive oils induce lysosomal membrane permeabilization in cancer cells. *PLoS ONE* **2019**, *14*, e0216024. [CrossRef] [PubMed]
24. Infante, R.; Infante, M.; Pastore, D.; Pacifici, F.; Chiereghin, F.; Malatesta, G.; Donadel, G.; Tesauro, M.; Della-Morte, D. An Appraisal of the Oleocanthal-Rich Extra Virgin Olive Oil (EVOO) and Its Potential Anticancer and Neuroprotective Properties. *Int. J. Mol. Sci.* **2023**, *24*, 17323. [CrossRef] [PubMed]
25. LeGendre, O.; Breslin, P.A.S.; Foster, D.A. (-)-Oleocanthal rapidly and selectively induces cancer cell death via lysosomal membrane permeabilization. *Mol. Cell. Oncol.* **2015**, *2*, e1006077. [CrossRef] [PubMed]
26. Chen, C.; Ai, Q.; Wei, Y. Potential role of hydroxytyrosol in neuroprotection. *J. Funct. Foods* **2021**, *82*, 104506. [CrossRef]
27. Fuccelli, R.; Fabiani, R.; Rosignoli, P. Hydroxytyrosol Exerts Anti-Inflammatory and Anti-Oxidant Activities in a Mouse Model of Systemic Inflammation. *Molecules* **2018**, *23*, 3212. [CrossRef] [PubMed]
28. Rafehi, H.; Smith, A.J.; Balcerczyk, A.; Ziemann, M.; Ooi, J.Y.; Loveridge, S.; Baker, E.; El-Osta, A.; Karagiannis, T. Investigation into the biological properties of the olive polyphenol, hydroxytyrosol: Mechanistic insights by genome-wide mRNA-Seq analysis. *Genes Nutr.* **2011**, *7*, 507–519. [CrossRef] [PubMed]
29. Reboredo-Rodríguez, P.; Varela-López, A.; Forbes-Hernández, T.Y.; Gasparrini, M.; Afrin, S.; Cianciosi, D.; Quiles, J.L.; Battino, M.; Giampieri, F. Phenolic Compounds Isolated from Olive Oil as Nutraceutical Tools for the Prevention and Management of Cancer and Cardiovascular Diseases. *Int. J. Mol. Sci.* **2018**, *19*, 2305. [CrossRef] [PubMed]
30. Gonçalves, M.; Vale, N.; Silva, P. Neuroprotective Effects of Olive Oil: A Comprehensive Review of Antioxidant Properties. *Antioxidants* **2024**, *13*, 762. [CrossRef] [PubMed]
31. Kusuma, I.Y.; Habibie, H.; Bahar, M.A.; Budán, F.; Csupor, D. Anticancer Effects of Secoiridoids—A Scoping Review of the Molecular Mechanisms behind the Chemopreventive Effects of the Olive Tree Components Oleocanthal, Oleacein, and Oleuropein. *Nutrients* **2024**, *16*, 2755. [CrossRef] [PubMed]

32. Torić, J.; Brozović, A.; Baus Lončar, M.; Jakobušić Brala, C.; Karković Marković, A.; Benčić, Đ.; Barbarić, M. Biological Activity of Phenolic Compounds in Extra Virgin Olive Oils through Their Phenolic Profile and Their Combination with Anticancer Drugs Observed in Human Cervical Carcinoma and Colon Adenocarcinoma Cells. *Antioxidants* **2020**, *9*, 453. [CrossRef] [PubMed]
33. Servili, M.; Esposto, S.; Fabiani, R.; Urbani, S.; Taticchi, A.; Mariucci, F.; Montedoro, G.F. Phenolic compounds in olive oil: Antioxidant, health, and organoleptic activities according to their chemical structure. *Inflammopharmacology* **2009**, *17*, 76–84. [CrossRef] [PubMed]
34. Hamdi, H.K.; Castellon, R. Oleuropein, a non-toxic olive iridoid, is an anti-tumor agent and cytoskeleton disruptor. *Biochem. Biophys. Res. Commun.* **2005**, *334*, 769–778. [CrossRef] [PubMed]
35. Omar, S.H. Cardioprotective and neuroprotective roles of oleuropein in Olive Oil. *Saudi Pharm. J.* **2010**, *18*, 111–121. [CrossRef] [PubMed]
36. Rishmawi, S.; Haddad, F.; Dokmak, G.; Karaman, R. A Comprehensive Review on the Anti-Cancer Effects of Oleuropein. *Life* **2022**, *12*, 1140. [CrossRef] [PubMed]
37. Martín-Peláez, S.; Covas, M.I.; Fitó, M.; Kušar, A.; Pravst, I. Health effects of olive oil polyphenols: Recent advances and possibilities for the use of health claims. *Mol. Nutr. Food Res.* **2013**, *57*, 760–771. [CrossRef] [PubMed]
38. Cornwell, D.G.; Ma, J. Nutritional Benefit of Olive Oil: The Biological Effects of Hydroxytyrosol and Its Arylating Quinone Adducts. *J. Agric. Food Chem.* **2008**, *56*, 8774–8786. [CrossRef] [PubMed]
39. Muriana, F.J.G.; Montserrat-de la Paz, S.; Lucas, R.; Bermudez, B.; Jaramillo, S.; Morales, J.C.; López, S. Tyrosol and its metabolites as antioxidative and anti-inflammatory molecules in human endothelial cells. *Food Funct.* **2017**, *8*, 2905–2914. [CrossRef] [PubMed]
40. Vázquez-Martín, A.; Fernández-Arroyo, S.; Cufí, S.; Oliveras-Ferraros, C.; Lozano-Sánchez, J.; Vellón, L.; Segura-Carretero, A.; Menéndez, J.A. Phenolic Secoiridoids in Extra Virgin Olive Oil Impede Fibrogenic and Oncogenic Epithelial-to-Mesenchymal Transition: Extra Virgin Olive Oil As a Source of Novel Antiaging Phytochemicals. *Rejuvenation Res.* **2012**, *15*, 1–13. [CrossRef] [PubMed]
41. Boskou, D. *Olive and Olive Oil Bioactive Constituents*; Academic Press: London, UK, 2015.
42. Fatoki, T.H.; Akintayo, C.O.; Ibraheem, O. Bioinformatics exploration of olive oil: Molecular targets and properties of major bioactive constituents. *OCL* **2021**, *28*, 36. [CrossRef]
43. Bulotta, S.; Celano, M.; Lepore, S.M.; Montalcini, T.; Pujia, A.; Russo, D. Beneficial effects of the olive oil phenolic components oleuropein and hydroxytyrosol: Focus on protection against cardiovascular and metabolic diseases. *J. Transl. Med.* **2014**, *12*, 219. [CrossRef] [PubMed]
44. Laveriano-Santos, E.; Vallverdú-Queralt, A.; Bhat, R.; Tresserra-Rimbau, A.; Lamuela-Raventós, R.M.; Pérez, M. Unlocking the potential of olive residues for functional purposes: Update on human intervention trials with health and cosmetic products. *J. Sci. Food Agric.* **2024**. [CrossRef] [PubMed]
45. Prodromou, S.I.; Chatzopoulou, F.; Saiti, A.; Giannopoulos-Dimitriou, A.; Koudoura, L.A.; Pantazaki, A.A.; Vasiliou, V.; Vizirianakis, I.S. Hepatotoxicity assessment of innovative nutritional supplements based on olive-oil formulations enriched with natural antioxidants. *Front. Nutr.* **2024**, *11*, 1388492. [CrossRef] [PubMed]
46. Quirantes-Piné, R.; Lozano-Sánchez, J.; Herrero, M.; Ibáñez, E.; Segura-Carretero, A.; Fernández-Gutiérrez, A. HPLC–ESI–QTOF–MS as a Powerful Analytical Tool for Characterising Phenolic Compounds in Olive-leaf Extracts. *Phytochem. Anal.* **2013**, *24*, 213–223. [CrossRef] [PubMed]
47. Dierkes, G.; Krieger, S.; Dück, R.; Bongartz, A.; Schmitz, O.J.; Hayen, H. High-performance liquid chromatography-mass spectrometry profiling of phenolic compounds for evaluation of olive oil bitterness and pungency. *J. Agric. Food Chem.* **2012**, *60*, 7597–7606. [CrossRef] [PubMed]
48. Cacciola, F.; Farnetti, S.; Dugo, P.; Marriott, P.; Mondello, L. Comprehensive two-dimensional liquid chromatography for polyphenol analysis in foodstuffs. *J. Sep. Sci.* **2017**, *40*, 7–24. [CrossRef] [PubMed]
49. Arena, K.; Cacciola, F.; Miceli, N.; Taviano, M.; Cavò, E.; Murphy, R.; Dugo, P.; Mondello, L. Determination of the polyphenolic content of berry juices using focusing-modulated comprehensive two-dimensional liquid chromatography coupled to mass spectrometry detection. *Anal. Bioanal. Chem.* **2022**, *414*, 6947–6959. [CrossRef] [PubMed]
50. Papakonstantinou, A.; Koumarianou, P.; Rigakou, A.; Diamantakos, P.; Frakolaki, E.; Vassilaki, N.; Magiatis, P.; Boleti, H. New Affordable Methods for Large-Scale Isolation of Major Olive Secoiridoids and Systematic Comparative Study of Their Antiproliferative/Cytotoxic Effect on Multiple Cancer Cell Lines of Different Cancer Origins. *Int. J. Mol. Sci.* **2023**, *24*, 3. [CrossRef] [PubMed]
51. Tutino, V.; Caruso, M.G.; Messa, C.; Perri, E.; Notarnicola, M. Antiproliferative, antioxidant and anti-inflammatory effects of hydroxytyrosol on human hepatoma HepG2 and Hep3B cell lines. *Anticancer Res.* **2012**, *32*, 5371–5377. [PubMed]
52. Papakonstatinou, A.; Koumarianou, P.; Diamantakos, P.; Melliou, E.; Magiatis, P.; Boleti, H. A Systematic Ex-Vivo Study of the Anti-Proliferative/Cytotoxic Bioactivity of Major Olive Secoiridoids' Double Combinations and of Total Olive Oil Phenolic Extracts on Multiple Cell-Culture Based Cancer Models Highlights Synergistic Effects. *Nutrients* **2023**, *15*, 2538. [CrossRef] [PubMed]

53. Cusimano, A.; Balasus, D.; Azzolina, A.; Augello, G.; Emma, M.R.; Di Sano, C.; Cervello, M. Oleocanthal exerts antitumor effects on human liver and colon cancer cells through ROS generation. *Int. J. Oncol.* **2017**, *51*, 533–544. [CrossRef] [PubMed]
54. Gabbia, D. Beneficial Effects of Tyrosol and Oleocanthal from Extra Virgin Olive Oil on Liver Health: Insights into Their Mechanisms of Action. *Biology* **2024**, *13*, 760. [CrossRef] [PubMed]
55. Saad, B.; Kmail, A. Olive Oil Polyphenols in Cancer: Molecular Mechanisms and Therapeutic Promise. *Immuno* **2025**, *5*, 36. [CrossRef]
56. Zubair, H.; Bhardwaj, A.; Ahmad, A.; Srivastava, S.; Khan, M.; Patel, G.; Singh, S.; Singh, A. Hydroxytyrosol Induces Apoptosis and Cell Cycle Arrest and Suppresses Multiple Oncogenic Signaling Pathways in Prostate Cancer Cells. *J. Nutr. Biochem.* **2017**, *48*, 9–18. [CrossRef] [PubMed]
57. Bektay, M.Y.; Güler, E.M.; Gökçe, M.; Kızıltaş, M.V. Investigation of the Genotoxic, Cytotoxic, Apoptotic, and Oxidant Effects of Olive Leaf Extracts on Liver Cancer Cell Lines. *Turk. J. Pharm. Sci.* **2021**, *18*, 781–789. [CrossRef] [PubMed]
58. Gorzynik-Debicka, M.; Przychodzen, P.; Cappello, F.; Kuban-Jankowska, A.; Gammazza, A.M.; Knap, N.; Gorska-Ponikowska, M. Potential Health Benefits of Olive Oil and Plant Polyphenols. *Int. J. Mol. Sci.* **2018**, *19*, 686. [CrossRef] [PubMed]
59. Paull, T.T. Mechanisms of ATM activation. *Annu. Rev. Biochem.* **2015**, *84*, 711–738. [CrossRef] [PubMed]
60. Vidal, A.E.; Boiteux, S.; Hickson, I.D.; Radicella, J.P. XRCC1 coordinates the initial and late stages of DNA abasic site repair through protein-protein interactions. *EMBO J.* **2001**, *20*, 6530–6539. [CrossRef] [PubMed]
61. Reczek, C.R.; Chandel, N.S. Two faces of reactive oxygen species in cancer. *Annu. Rev. Cancer Biol.* **2016**, *1*, 79–98. [CrossRef] [PubMed]
62. Zou, X.; Ratti, B.A.; O'Brien, J.; Silva, S.D.; Gius, D.; Bonini, M.; Zhu, Y. Manganese superoxide dismutase (SOD2): Is there a center in the universe of mitochondrial redox signaling? *J. Bioenerg. Biomembr.* **2017**, *49*, 325–333. [CrossRef] [PubMed]
63. Xu, J.; Wei, H.; Sun, Z.; Li, W.; Long, J.; Liu, J.; Feng, Z.; Cao, K. Hydroxytyrosol as a Mitochondrial Homeostasis Regulator: Implications in Metabolic Syndrome and Related Diseases. *Antioxidants* **2025**, *14*, 398. [CrossRef] [PubMed]
64. Choi, S.; Joo, H.; Jeon, B. Dynamic Regulation of APE1/Ref-1 as a Therapeutic Target Protein. *Chonnam Med. J.* **2016**, *52*, 75–80. [CrossRef] [PubMed]
65. García-Martínez, O.; Luna-Bertos, E.; Ramos-Torrecillas, J.; Ruíz, C.; Milia, E.; Lorenzo, M.; Jiménez, B.; Sánchez-Ortíz, A. Rivas, Phenolic Compounds in Extra Virgin Olive Oil Stimulate Human Osteoblastic Cell Proliferation. *PLoS ONE* **2016**, *11*, e0150045. [CrossRef] [PubMed]
66. Camargo, A.; Ruano, J.; Fernández, J.; Parnell, L.D.; Jiménez, A.; Santos-González, M.; Pérez-Jiménez, F. Gene expression changes in mononuclear cells in patients with metabolic syndrome after acute intake of phenol-rich virgin olive oil. *BMC Genom.* **2010**, *11*, 253. [CrossRef] [PubMed]
67. Aziz, H.; Zaas, A.; Ginsburg, G.S. Peripheral blood gene expression profiling for cardiovascular disease assessment. *Genom. Med.* **2007**, *1*, 105–112. [CrossRef] [PubMed]
68. Nasrallah, N.A.; Zhou, H.; Smith, P.A.; Sears, C.R. DNA Repair Capacity for Personalizing Risk and Treatment Response-Assay Development and Optimization in Human Peripheral Blood Mononuclear Cells (PBMCs). *DNA Repair* **2022**, *111*, 103274. [CrossRef] [PubMed]
69. Dong, C. Cytokine regulation and function in T cells. *Annu. Rev. Immunol.* **2021**, *39*, 51–76. [CrossRef] [PubMed]
70. Angerfors, A.; Lindvall, M.; Andersson, B.; Nilsson, S.; López, M.; Hansson, L.; Jern, C. Comparison of DNA Methylation Profiles of Hemostatic Genes between Liver Tissue and Peripheral Blood within Individuals. *Thromb. Haemost.* **2020**, *120*, 1737–1748. [CrossRef] [PubMed]
71. Zhu, W.; Zhang, Q.; Liu, M.; Yan, M.; Chu, X.; Li, Y. Identification of DNA repair-related genes predicting pathogenesis and prognosis for liver cancer. *Cancer Cell Int.* **2021**, *21*, 79. [CrossRef] [PubMed]
72. Zhang, C.; Guo, X.; Liu, P.; Wang, Y.; Zhang, J.; Li, L.; Wang, Z. The neuro-immune axis in cancer: From mechanisms to therapeutic opportunities. *J. Hematol. Oncol.* **2025**, *18*, 48. [CrossRef] [PubMed]
73. Xia, L.; Oyang, L.; Lin, J.; Tan, S.; Han, Y.; Wu, N.; Liao, Q. The cancer metabolic reprogramming and immune response. *Mol. Cancer* **2021**, *20*, 92. [CrossRef] [PubMed]
74. Karagiannis, P.; Takahashi, K.; Saito, M.; Yoshida, Y.; Okita, K.; Yamanaka, S.; Osafune, K. Induced Pluripotent Stem Cells and Their Use in Human Models of Disease and Development. *Physiol. Rev.* **2018**, *98*, 79–114. [CrossRef] [PubMed]

Disclaimer/Publisher's Note: The statements, opinions and data contained in all publications are solely those of the individual author(s) and contributor(s) and not of MDPI and/or the editor(s). MDPI and/or the editor(s) disclaim responsibility for any injury to people or property resulting from any ideas, methods, instructions or products referred to in the content.